Behavioral/Cognitive

Metabotropic NMDAR Signaling Contributes to Sex Differences in Synaptic Plasticity and Episodic Memory

Aliza A. Le,[1] Julie C. Lauterborn,[1] Yousheng Jia,[1] Conor D. Cox,[1] Gary Lynch,[1,2] and Christine M. Gall[1,3]
Departments of [1]Anatomy and Neurobiology, [2]Psychiatry and Human Behavior, and [3]Neurobiology and Behavior, University of California, Irvine, California 92697

NMDA receptor (NMDAR)-mediated calcium influx triggers the induction and initial expression of long-term potentiation (LTP). Here we report that in male rodents, ion flux-independent (metabotropic) NMDAR signaling is critical for a third step in the production of enduring LTP, i.e., cytoskeletal changes that stabilize the activity-induced synaptic modifications. Surprisingly, females rely upon estrogen receptor alpha (ERα) for the metabotropic NMDAR operations used by males. Blocking NMDAR channels with MK-801 eliminated LTP expression in hippocampal field CA1 of both sexes but left intact theta burst stimulation (TBS)-induced actin polymerization within dendritic spines. A selective antagonist (Ro25-6981) of the NMDAR GluN2B subunit had minimal effects on synaptic responses but blocked actin polymerization and LTP consolidation in males only. Conversely, an ERα antagonist thoroughly disrupted TBS-induced actin polymerization and LTP in females while having no evident effect in males. In an episodic memory paradigm, Ro25-6981 prevented acquisition of spatial locations by males but not females, whereas an ERα antagonist blocked acquisition in females but not males. Sex differences in LTP consolidation were accompanied by pronounced differences in episodic memory in tasks involving minimal (for learning) cue sampling. Males did better on acquisition of spatial information whereas females had much higher scores than males on tests for acquisition of the identity of cues (episodic "what") and the order in which the cues were sampled (episodic "when"). We propose that sex differences in synaptic processes used to stabilize LTP result in differential encoding of the basic elements of episodic memory.

Key words: **actin; estrogen receptor; hippocampus; memory; metabotropic; NMDAR**

Significance Statement

Calcium influx through NMDARs has long been recognized as the initiating event for LTP. Results of the present studies call for a substantial revision to this fundamental observation about learning-related synaptic plasticity. Specifically, we show cytoskeletal mechanisms that consolidate field CA1 LTP and episodic memory are triggered not by NMDAR-mediated calcium but by ion flux-independent (metabotropic) signaling. Males use metabotropic functions of the NMDARs for this purpose whereas females rely upon synaptic estrogen receptors. This unprecedented instance of sex differences in synaptic function is accompanied by surprisingly large male/female differences in the acquisition of the three basic elements of episodic memory.

Introduction

NMDA receptors (NMDARs) are unusual in that opening of their channel requires both ligand binding and prolonged depolarization. These arrangements result in a type of "coincidence detector" (Seeburg et al., 1995; Dore et al., 2017) that is engaged by co-occurrence of presynaptic (release) and postsynaptic (depolarization) events. This discovery was of great interest because theorists had proposed that synchronized activity by inputs and target cells strengthens synaptic contacts whereas uncoordinated firing reduces synaptic strength (Hebb, 1949; Lisman et al., 2011; Markram et al., 2011; Baldi and Vershynin, 2021). NMDARs fit naturally into this scheme because they require transmitter binding and spine depolarization before gating calcium into spines, an event that is essential for shifting synapses into their potentiated state (Lynch et al., 1983; Paoletti et al., 2013; Volianskis et al., 2013). However, there is increasing evidence that NMDARs also signal in an ion flux-independent, or metabotropic (m-), manner (Brunetti et al., 2024). NMDAR-driven

Received Feb. 21, 2024; revised Oct. 2, 2024; accepted Oct. 3, 2024.
Author contributions: A.A.L., J.C.L., Y.J., G.L., and C.M.G. designed research; A.A.L., J.C.L., and Y.J. performed research; A.A.L., J.C.L., Y.J., and C.D.C. analyzed data; A.A.L., J.C.L., G.L., and C.M.G. wrote the paper.
This work was funded by the Eunice Kennedy Shriver National Institute of Child Health and Human Development Grant HD089491, National Institute on Drug Abuse Grant DA044118, Office of Naval Research Grant N00014-21-1-2940, National Science Foundation Grant BCS-1941216, National Institute of Mental Health Training Grant T32-MH119049.
The authors declare no competing financial interests.
Correspondence should be addressed to Christine M. Gall at cmgall@uci.edu or Gary Lynch at g.as.lynch@gmail.com.
https://doi.org/10.1523/JNEUROSCI.0438-24.2024

processes including long-term depression (LTD; Nabavi et al., 2013; Dore et al., 2015), spine shape change (Birnbaum et al., 2015; Stein et al., 2021), and excitotoxic damage (Weilinger et al., 2016; Li et al., 2022) are reportedly unaffected by agents (e.g., MK-801) that block the receptor's ion channel. In contrast, field CA1 long-term potentiation (LTP) is entirely suppressed by MK-801 (Coan et al., 1987; Frankiewicz et al., 1996), and there is no evidence that the brief, learning-related activity patterns used to induce potentiation actually engage m-NMDAR signaling.

Surprisingly little is known about NMDAR operations in females, an oversight that is of particular interest given recent reports documenting striking sex differences in LTP substrates (Jain et al., 2019; Gall et al., 2021). NMDARs are essential for the postsynaptic mechanisms of LTP in the CA3→CA1, Schaffer-commissural (SC) projections in both sexes but only females also require locally produced estrogen acting on synaptic estrogen receptors to stabilize potentiation (Kramár et al., 2009; Vierk et al., 2012; W. Wang et al., 2018a). Thus, the question of whether nonionotropic NMDAR functions contribute to LTP needs to be broadened to include the possibility that there are sex differences in reliance upon such mechanisms.

Likely related to sexually differentiated estrogen involvement, the induction threshold for CA1 LTP is higher in adult females than that in males (W. Wang et al., 2018a; Le et al., 2022b). This helps explain reported sex differences in hippocampus-dependent memory including evidence that males typically score better on spatial tasks (Andreano and Cahill, 2009; Barel and Tzischinsky, 2018; Le et al., 2022b). Although this aligns with sex differences in LTP thresholds, in other instances the relationship is unclear. Specifically, women frequently have higher scores for verbal learning and for components of episodic memory (Herlitz et al., 1999; Asperholm et al., 2019; Jensen et al., 2023) that depend on the hippocampus (Noulhiane et al., 2007; Dede et al., 2016). Corresponding tests for sex differences in episodic memory in rodents are lacking.

The present studies tested if m-NMDAR functions contribute to SC LTP and episodic memory. Prior work has shown that LTP-inducing theta burst stimulation (TBS) activates multiple synaptic signaling cascades (El Gaamouch et al., 2012; W. Wang et al., 2018a; Gall et al., 2021) leading to the formation and stabilization of filamentous-actin (F-actin; Lin et al., 2005; Kramár et al., 2006). This postsynaptic F-actin remodeling is required for consolidation of recently induced SC LTP in males and females (Krucker et al., 2000; Kramár et al., 2006; Rex et al., 2009; W. Wang et al., 2018a). We tested here if nonionotropic functions of the NMDAR are critical for TBS-induced SC LTP, actin regulatory signaling, and increases in F-actin in both sexes. Studies further assessed the involvement of the NMDAR GluN2B subunit implicated in m-NMDAR functions (Y. Li et al., 2022). The results demonstrate striking sex differences in m-NMDAR control of cytoskeletal mechanisms that consolidate LTP and opened the way for tests of sexually differentiated contributions of m-NMDAR signaling to episodic memory. Finally, we investigated the possibility that sex differences in LTP substrates are accompanied by differences in acquisition of the distinct components of episodic memory (Tulving, 1984) and specifically the identities, locations, and temporal order (What, Where, and When information) for a collection of cues.

Materials and Methods

Animals. Experiments used 2–4-month-old Sprague Dawley rats (Charles River Laboratories) and 2–4-month-old sighted-FVB129 mice (in-house colony) of both sexes. Animals were group housed (rat, 2–4/cage; mice, 3–5/cage) in rooms with 12 h light/dark cycle (lights on 6:30 A.M.; 68°F, 55% humidity) and food/water *ad libitum*. Rats were acclimated to the vivarium for a minimum of 3 d prior to experimental use. Experiments were conducted in accordance with the National Institutes of Health Guide for the Care and Use for Laboratory Animals and protocols approved by the Institutional Animal Care and Use Committee at the University of California, Irvine.

Field electrophysiology. To minimize potential effects of stress, animals were quickly anesthetized with isoflurane and promptly decapitated. Hippocampal slices were prepared from 2–4-month-old male and female rats using a McIllwain tissue chopper (370 µm; transverse) and immediately transferred to an interface recording chamber with continuous perfusion of oxygenated artificial cerebrospinal fluid (aCSF; 60–70 ml/h, 31 ± 1°C, 95% O_2/5% CO_2) that included the following (in mM): 124 NaCl, 26 $NaHCO_3$, 3 KCl, 1.25 KH_2PO_4, 2.5 $CaCl_2$, 1.5 $MgSO_4$, and 10 dextrose, pH 7.4. Experiments were initiated 2 h later. The analysis focused on Schaffer-commissural (SC) afferents to field CA1b stratum radiatum (SR), a system for which postsynaptic mechanisms of LTP (Granger and Nicoll, 2014; Gall et al., 2024) and sex differences in estrogen involvement in potentiation (Vierk et al., 2012; W. Wang et al., 2018a; Jain et al., 2019; Le et al., 2022b) are well documented. Field excitatory postsynaptic potentials (fEPSPs) were elicited using a twisted nichrome wire stimulating electrode in CA1a or CA1c SR and recorded with a glass pipette electrode (filled with 2 M NaCl; $R = 2–3$ MΩ) in CA1b SR. Single-pulse baseline stimulation was applied with fEPSP amplitude at ∼40–50% of the maximum population spike-free amplitude. Responses were digitized at 20 kHz using an AC amplifier (A-M Systems, Model 1700) and recorded using NAC2.0 Neurodata Acquisition System (Theta Burst Corporation).

Unless otherwise stated, both short-term potentiation (STP; i.e., the mean response over the first three pulses post-TBS normalized to the mean baseline response) and LTP (i.e., the mean response during last 5 min post-TBS, normalized to the mean baseline response) were induced using a 10-burst train of TBS (four pulses at 100 Hz per burst, 200 ms between bursts). A single train of TBS was selected because it mimics the natural firing pattern in CA1 stratum pyramidale (SP) neurons of behaving animals (Otto et al., 1991), elicits reliable and enduring LTP in slices from adult male and female rodents (Larson et al., 1986; Staubli and Lynch, 1987; Larson and Lynch, 1988; Kramár et al., 2009; Kouvaros and Papatheodoropoulos, 2016; Le et al., 2022b), and elicits NMDAR-dependent LTP while avoiding calcium contributions from voltage-gated calcium channels and other sources that are observed with LTP induction using either high frequency stimulation or repeated bouts of TBS (Raymond, 2007; Kouvaros and Papatheodoropoulos, 2016; Papatheodoropoulos and Kouvaros, 2016). Moreover, this induction paradigm was used in numerous studies evaluating the mechanisms and critical function of NMDAR-dependent spine actin remodeling for the stabilization of CA3-CA1 LTP (Lin et al., 2005; Kramár et al., 2006; Rex et al., 2007, 2009, 2010; Chen et al., 2010a; Babayan et al., 2012) as well as investigations of estrogen receptor involvement in actin regulatory signaling (Kramár et al., 2009; W. Wang et al., 2018a). To identify contributions of specific receptors in LTP, additional studies used a stimulation paradigms that was found to be near threshold for induction in prior work (W. Wang et al., 2018a; Le et al., 2022b): i.e., TBS triplets were applied four times spaced by 90 s. Drugs were infused into the slice bath beginning 1–2 h before TBS unless otherwise stated.

Whole-cell current clamp. Hippocampal slices (350 µm, transverse) from 2-month-old male mice were prepared using a Leica Vibroslicer (VT1000S) and placed in a submerged recording chamber with constant oxygenated aCSF perfusion (2 ml/min) at 32°C. Whole-cell recordings (Axopatch 200A amplifier, Molecular Devices) used 4–7 MΩ glass pipettes filled with the following (in mM): 140 $CsMeSO_3$, 8 CsCl, 10 HEPES, 0.2 EGTA, 2 QX-314, 2 Mg-ATP, 0.3 Na-GTP. Tungsten concentric bipolar stimulating electrodes (6 µm diameter; World Precision Instruments) were placed in the CA1 SR, 100–150 µm from the recorded cell located in CA1b SP. Excitatory postsynaptic currents (EPSCs) were

recorded with the holding potential at +40 mV for NMDAR amplitude (at 50 ms from stimulation artifact) in the presence of 50 μM picrotoxin. Data were collected using Clampex 10.6 and analyzed with Clampfit 10.6 (Molecular Devices).

Fluorescence deconvolution tomography. For measures of basal synaptic protein levels, hippocampal slices (370 μm) were immersed in 4% paraformaldehyde (PFA, 4°C) overnight. For LTP experiments, electrodes were placed in CA1a and CA1c SR for stimulation and CA1b SR for recording, all equidistant from the cell layer. After ∼5 min of stable baseline, one TBS train was applied to each polarity of each stimulating electrode (pulses at 2× baseline duration). Control slices received continuous 3/min single-pulse stimulation (referred to as baseline control or low-frequency stimulation). Slices were harvested at a specified time post-TBS [3 min for analysis of phosphorylated (p) ERK (W. Wang et al., 2018a), 7 min for pSrc (Chen et al., 2010b), and 15 min for pCAMKII (C. D. Cox et al., 2014)] and fixed in PFA overnight. Slices were subsectioned (20 μm) and 6–8 sections from the top (interface plane) of each slice were slide mounted and processed for dual immunofluorescence as described (Seese et al., 2012; W. Wang et al., 2018a).

The following primary antibodies (concentration; vendor, catalog #, RRID) were used: goat anti-PSD95 (1:1,500; Abcam, ab12093, AB_298846) with either rabbit anti-pCaMKII T286/T287 [1:500; Upstate (now Millipore), 06-881, AB_310282] or rabbit anti-pERK1/2 T202/Y204 (1:500; Cell Signaling 4377, AB_331775); Mouse anti-PSD95 (1:1,000; Invitrogen, MA1-045, AB_325399) with rabbit anti-pSrc Y419 (1:250; Invitrogen, 44-660G, AB_2533714); Rabbit anti-GluN1 (extracellular) (1:1,000; Alomone Labs, AGC-001, AB_2040023), anti-GluN2A (1:500, Alomone Labs, AGC-002, AB_2040025), anti-GluN2B (1:500, Alomone Labs, AGC-003, AB_2040028), or anti-GluN2B Y1472 (1:300; PhosphoSolutions, P1516-1472, AB_2492182) with goat anti-PSD95 (1:1,500, Abcam, ab12093, AB_298846). Secondary antibodies (all at 1:1,000, Invitrogen) included Alexa Fluor donkey anti-goat 488 (A32814, AB_2762838), donkey anti-rabbit 594 (A32754, AB_2762827), donkey anti-mouse 594 (A21203, AB_141633), and donkey anti-rabbit 488 (A21206, AB_2535792).

Fluorescence deconvolution tomography (FDT) was used to quantify synaptic protein levels as described (Rex et al., 2009; Babayan et al., 2012; Seese et al., 2014; W. Wang et al., 2018a). This approach has the advantage of measuring the incidence and immunofluorescence intensity of over 20,000 individually evaluated postsynaptic elements (i.e., those immunolabeled for the excitatory synapse scaffold protein PSD95) for each image *z*-stack and thus for over 100,000 synapses per hippocampal slice. Moreover, the analysis of double labeling is evaluated from three-dimensional (3-D) reconstructions of the *z*-stack, thus assuring there is real contact or overlap in the fields of labeling by the different fluorophores. Briefly, image *z*-stacks (136 × 105 × 2 μm, 200 nm steps; 0.103 μm/pixel; 63× capture) were collected from the CA1 apical dendritic field SR, at the same distance from SP as the stimulation electrodes, from ≥5–7 sections per hippocampal slice and processed for iterative deconvolution (99% confidence; Volocity 4.0, PerkinElmer). 3-D montages of each *z*-stack were then analyzed for synaptic labeling using in-house software [c99, Java (OpenJDK IcedTea 6.1.12.6), Matlab R2019b, PuTTY 0.74, and Perl 5.30.0]. Each image was converted to 8 bit, and the background was normalized using a Gaussian blur to reduce the impact of background intensity variations across the image. Images were then processed through a fixed series of intensity thresholds to identify the immunofluorescence intensity of the labeled profiles. Erosion and dilation filtering was used to fill holes and remove background pixels to detect edges of both faintly and densely labeled structures. Objects were then segmented based on connected pixels above a threshold across each channel separately. All immunofluorescent elements meeting size constraints (0.04–1.2 μm^2) and eccentricity (<2) of synapses, and detected across multiple thresholds, were quantified. PSD95-immunoreactive (IR) elements were considered double-labeled if there was contact or overlap in fields occupied by the two fluorophores as assessed in 3-D. Approximately 20,000–30,000 synapses were thus analyzed per *z*-stack. Based on the maximum intensity of each image, counts of double-labeled puncta were assigned to ascending density (fluorescence intensity) bins, and the data were expressed as density frequency distribution histograms. Labeled puncta with immunofluorescence density at ≥95 on the arbitrary 255 step scale were considered densely labeled. Counts of densely labeled puncta for each section were averaged with those from other sections of the same slice to generate the mean slice value presented. Graphs show group mean ± SEM values.

In situ F-actin phalloidin labeling. As described previously (Lynch et al., 2007; Rex et al., 2007), Alexa Fluor 568-conjugated phalloidin (Invitrogen; A12380) was diluted in water to 12 μM stock and then to 6 μM in aCSF (1% DMSO) prior to experimentation. Electrode placement and stimulation was as for FDT analyses. Beginning 3 min post-stimulation, phalloidin (6 μM, 2 μl) was applied topically onto the slice (3 times, 3 min apart). Three minutes after the last application, slices were fixed in cold 4% PFA overnight. After cryoprotection (20% sucrose in 4% PFA), slices were subsectioned, slide mounted, washed in 0.1 M phosphate buffer (PB; 10 min), and coverslipped with Vectashield containing DAPI (VectorLabs). To quantify spine phalloidin labeling, image *z*-stacks (136 × 105 × 3 μm) were captured as for FDT. Every image of each *z*-stack then received a small saturated 1 × 1 μm reference square to two corners of the image (Python 3.0). The global reference square adds a fixed maximum intensity level for all images without significantly altering the background or raw intensity values of phalloidin-labeled puncta; this step was added because the software assigns the final density values for phalloidin labeling based on the maximum intensity of a given image. The image *z*-stacks were then processed for quantification of spine-sized puncta as described for FDT; labeled puncta within the density bins of ≥90 were considered to have dense concentrations of F-actin. Counts of densely labeled puncta were then averaged across tissue sections to generate a mean ± SEM value per slice. Values from experimental groups were normalized to those of their respective control group.

Behavioral assays. To assess effects of sex and ion flux-independent NMDAR function on acquisition of the components of episodic memory (i.e., "What," "When," and "Where" information), mice were tested in unsupervised tasks that used multiple odor cues and did not involve repetition or reward (W. Wang et al., 2018b; B. M. Cox et al., 2019; Le et al., 2022b). These tasks are similar to other episodic memory paradigms that used object cues (Dere et al., 2005a, b) but differ in using both a greater number of cues, presented in series or simultaneously, and odors as cues. Odors were selected because they are of innate interest to macrosmatic animals such as rodents. Two different behavioral arenas were employed. The Serial "What" and "When" tasks (described below) used opaque plexiglass arenas (30 × 25 cm floor, 21.5 cm height) into which two identical jars were placed in diagonally opposite corners (1 inch away from the walls) for cue presentation. The Simultaneous "What" and "Where" tasks (see below) employed a larger arena (60 × 60 cm floor, 30 cm height) with four identical jars positioned in each corner, 1 inch away from the walls. In all cases, the jars were placed into small recesses (∼1 cm) in the arena floor to assure that the cues were presented in the same location in each session. Each jar (5.2 cm diameter, 5 cm tall) had a 15 mm hole in the center of the lid to allow for odor sampling. All odorants were dissolved in mineral oil to achieve a final concentration of 0.1 Pa, and 100 μl was pipetted onto a filter paper that was placed at the bottom of the jar (beyond animal access); each odorant was presented in its own jar and clean jars were used for each odor presentation. The following odors, with letter identification, were used: (A) (+)-limonene (≥97% purity, Sigma-Aldrich), (B) cyclohexyl ethyl acetate (≥97%, International Flavors & Fragrances), (C) (+)-citronellal (∼96% Alfa Aesar), (D) octyl aldehyde (∼99%, Acros Organics), (E) anisole (∼99% Acros Organics). These odors were previously found to be of comparable interest, as determined by relative amount of time spent exploring the cue, to male and female mice (Le et al., 2022b). The arenas were wiped down with ethanol between animals on a given day and were thoroughly cleaned between experimental days. In all cases the mice were handled for 2 min the day before experimentation to reduce anxiety and were allowed to explore the arena with unscented jars present for 5 min prior to first odor exposure. For all trials, animal movements were recorded using overhead cameras for later quantification of odor

exploration by persons blind to group and movements via Ethovision NT.

Serial "What" task. To assess the acquisition of cue identity ("What"), mice were exposed to a series of identical odor pairs and then, at retention testing, the animals were again presented with two cues, one from the original series and the other being a novel odor (A:D). As rodents have a strong preference for investigating novel stimuli (Dere et al., 2005a), they typically spend more time investigating a novel cue relative to a familiar, previously sampled cue (W. Wang et al., 2018b; B. M. Cox et al., 2019). Initially, each mouse was allowed to explore an arena containing two unscented jars for 5 min. The jars were removed and the animal remained in the arena for 5 min. Mice were then presented with a series of odorant pairs (A:A > B:B > C:C) for 3 min each and 5 min between pairs. After a 5 min delay following the last sample presentation (C:C), the mouse was presented with the test odorant pair A:D and was allowed to explore for 5 min; the locations of odors A and D were counterbalanced across these test trials. The time spent exploring the odors was quantified for all odor presentations. Greater time sampling novel odor D versus previously presented odor A at testing was interpreted as evidence that the animal discriminated the novel from the familiar cue and thus had acquired the identity of the familiar cue. For the four-odor version of this task, an additional odor pair was added to the initial sample sequence (A:A > B:B > C:C > D:D) and mice were presented with novel odor E and previously sampled odor A (A:E) at testing. This four-odor task was counterbalanced at testing by using odor D first, and odor A last, in the sample series (D:D > B:B > C:C > A:A followed by D:E at testing).

Serial "When" task. This task tests if the animal distinguishes the temporal order of cues sampled within an odor series and thus discriminates (preferentially explores) a cue encountered earlier in that series from a cue presented later in that series (B. M. Cox et al., 2019). This task used exposure to same four-odor sequence as above (A:A > B:B > C:C > D:D; 3 min each/5 min spacing) but, in this instance, at testing the mice were presented with a pair of familiar odors including the first (A) and second (B) odors in the prior sampling sequence for 5 min [similar to the "temporal order" task of Dere et al. (2005b)]. We previously demonstrated that adult male mice discriminate and preferentially explore less recent, familiar odor B versus more-recent familiar odor C in studies using this design and that performance in this Serial "When" task was impaired by unilateral silencing of field CA3 whereas performance on "What" and "Where" tasks were not (B. M. Cox et al., 2019).

Simultaneous "What" task. The mice were initially placed in the arena containing four unscented jars for 5 min. The jars were removed and then, after a 3 min delay, were replaced with jars containing four different odors (A:B:C:D) placed at the same fixed positions near the corners of the arena; during this exposure session, the mice were allowed to freely explore the arena and sample odors for 5 min after which they were returned to their home cages. At retention testing 48 h later, the mice were reintroduced to the chamber containing three of the initial cues (A:B:C) placed in their original locations and one novel cue (E) that supplanted odorant D's location. They were allowed to freely explore for 5 min.

Simultaneous "Where" task. For this task the arena habituation and initial odor sampling session was the same as for the simultaneous "What" task (above). Five minutes after the initial odor exposure session, during which the mice remained in the arena without scented jars, the odors were reintroduced but with the position of two odorants initially placed in opposite corners (e.g., pair A:D or B:C) swapped. The other cue locations were unchanged. The mice were then allowed to freely explore the arena for 5 min. Note: To assess drug effects on "Where" task performance, the initial odorant exposure session was extended to 10 min to allow both sexes to learn (Le et al., 2022b), and retention was tested 24 h later. Prior studies have shown that bilateral silencing of medial entorhinal cortex, and its input to the hippocampus, impairs performance on this "Where" task without effect on performance in the serial "What" and "When" tasks (B. M. Cox et al., 2019).

Behavioral scoring. All behavioral sessions were digitally recorded using an overhead camera and behavior was scored, for time the animal spent exploring the scented jars, from the digital recordings by observers blind to group. For scoring in the serial "What" and "When" tasks, sampling was quantified for a 3 min period beginning from when the animal sampled one of the cues for the first time. For the Simultaneous "What" and "Where" task, cue sampling was scored for the full 5 min test period. In all cases, cue sampling time (t) was collected as the number of seconds the mouse's nose was actively pointed toward, and within 0.5 cm of the hole in the scent jar lid, including time dipping their nose into the hole. Incidental head turning within the zone was not included in the scoring. Predetermined criteria for excluding animals from analyses included (1) exploration of any odor for <1 s or (2) excessively chewing the jar lids: no mice were excluded based on these criteria. Calculations for the discrimination index (DI) across the tasks were as follows: "Where" $DI = 100 \times (t_{\text{sum of switched pair}} - t_{\text{sum of stationary pair}}) / (t_{\text{total sampling}})$; serial "What" and "When" $DI = 100 \times (t_{\text{novel}} - t_{\text{familiar}}) / (t_{\text{total sampling}})$; simultaneous "What" $DI = 100 \times (t_{\text{novel}} - t_{\text{mean familiars}}) / (t_{\text{total sampling}})$. Z-score calculations were as follows: $(\text{mean } DI_{\text{female}} - \text{mean } DI_{\text{male}}) / (\text{standard deviation}_{\text{male}})$.

Drug administration. For behavior, Ro25-6981 (Ro25; 5 mg/kg, saline) and methyl-piperidino-pyrazole (MPP; 0.6 mg/kg, 2% DMSO in saline) were injected intraperitoneally 30 and 60 min before exposure to odors, respectively. For electrophysiology, compounds were introduced to the slice bath via a syringe pump (6 ml/h; KD Scientific, model 100) into the aCSF infusion line for the following final bath concentrations: MK-801 (30 μM; Tocris, 0924), APV (100 μM; Hello Bio, HB0225), DNQX (20 μM; Hello Bio, HB0261), picrotoxin (30 μM; Sigma-Aldrich, P1675), MPP dihydrochloride (MPP; 3 μM; Tocris, 1991), and Ro25-6981 (3 μM; Hello Bio, HB0554). MPP and Ro25 were initially dissolved in DMSO; the final bath concentration of DMSO was ≤0.01%. Other compounds were initially dissolved in water.

Software accessibility. The data supporting the findings of this study are available from the corresponding author upon reasonable request. Theta burst areas for field electrophysiology were analyzed using code available at https://github.com/cdcox/Theta-burst-analyzer-for-Le-et-al. Code for FDT analysis is made available upon request. The use of the FDT code is strictly prohibited without a Licensing Agreement from The University of California, Irvine.

Experimental design and statistical analysis. Mice were used for behavioral experiments because the paradigms were developed in mice in studies that determined that the odor cues employed are balanced for interest in male and females, identified training periods that support (and are near threshold for) acquisition of the different components of episodic memory, and determined that there are differences in the hippocampal subfields that are critical for acquisition of the different components of episodic memory (W. Wang et al., 2018b; B. M. Cox et al., 2019; Le et al., 2022a; Brunetti et al., 2024). Rats were used for electrophysiology (except for analysis in Fig. 2*C*) and for immunolabeling experiments because their larger hippocampus allowed for precise targeting of specific laminae for stimulation and microscopic analyses, immunofluorescence, and in situ phalloidin labeling procedures were devised in studies of rat, and some of the antisera are better suited to labeling the rat protein sequence (Kramár et al., 2006; Rex et al., 2007, 2009; W. Wang et al., 2018a). A reliance on F-actin remodeling for the consolidation of LTP has been demonstrated in both rats (Kramár et al., 2006; Rex et al., 2010; Babayan et al., 2012) and mice (Krucker et al., 2000; Kelly et al., 2007; Baudry et al., 2012). Males and females were used for all experiments except the whole-cell recordings which focused on males. Females were estrous staged (Le et al., 2022b) and used outside proestrus (i.e., were used in estrus and diestrus 1,2) to avoid the transient proestrus peak in circulating and hippocampal estrogen levels and the associated effect on learning behavior (Tuscher et al., 2015; Hojo and Kawato, 2018; W. Wang et al., 2018a). The NMDAR subunit analysis used diestrus females to minimize variability that has been described across estrous stages (B. Tang et al., 2008; Smith et al., 2016). For

electrophysiology and microscopy experiments, *N* denotes the number of hippocampal slices from ≥3 animals.

Significance ($p < 0.05$) was determined using GraphPad Prism (v6.0); details of all statistical analyses (*p* values, degrees of freedom, and *t* tests) are presented in Extended Data Figure 1-1. For electrophysiological experiments, the magnitudes of LTP (averaged fEPSP slopes for the last 5 min of recordings, normalized to the mean baseline response over 20 min prior to TBS) and STP (mean response over 1 min post-TBS, normalized to baseline) were compared via the two-tailed unpaired Student's *t* test. TBS area analysis and STP (for threshold TBS) were analyzed with repeated-measures two-way ANOVA. For imaging and behavioral studies, two-tailed unpaired Student's *t* test or Mann–Whitney *U* test, if data did not pass the *F* test for variance, was employed for comparing two groups. Significance for ≥3 group comparisons was assessed using one- and two-way ANOVA (post hoc Tukey's test) or the Kruskal–Wallis test (post hoc Dunn) as dictated by outcome of the Brown–Forsythe test for variance.

Results

Blocking the NMDAR channel does not interfere with TBS-induced LTP or actin polymerization in males

The evaluation of m-NMDAR involvement in LTP focused on SC innervation of apical field CA1, the system for which contributions of nonionotropic NMDAR signaling to LTD, bidirectional structural plasticity, and deleterious actions of Aß have been described (Nabavi et al., 2013; Birnbaum et al., 2015; Stein et al., 2015, 2021). Moreover, mechanisms of LTP, including cytoskeletal involvement in stabilization machinery, are well characterized for this system (Krucker et al., 2000; Rex et al., 2010; Gall et al., 2021). The latter studies have shown that TBS of the SC projections causes a rapid and lasting increase in filamentous (F-) actin in dendritic spines in CA1 stratum radiatum (SR) and that blocking this F-actin increase prevents LTP stabilization (Krucker et al., 2000; Lin et al., 2005; Kramár et al., 2006; Ramachandran and Frey, 2009; Bosch et al., 2014; H. Wang and Peng, 2016). We first tested, in adult male hippocampal slices, if SC LTP and activity-driven increases in spine F-actin require NMDAR-mediated ion flux by infusing MK-801, a noncompetitive antagonist that occludes the NMDAR ion channel without interfering with glutamate binding to the receptor (Song et al., 2018). Application of a single 10-burst train of TBS elicited robust LTP in control, vehicle-treated, slices whereas MK-801 (30 μM) infusion initiated 2 h prior to application of the theta train produced a near complete suppression of both the initial short-term potentiation (STP) and LTP (Fig. 1*a*; Extended Data Fig 1-1) as expected from prior work (Frankiewicz et al., 1996). To evaluate effects on actin polymerization, a single train of TBS was applied to two populations of CA3 efferents converging on the apical dendrites of CA1b pyramidal cells, with a 30 s delay between activation of the distinct inputs (Fig. 1*b*). Alexa Fluor 568-phalloidin, which selectively binds F-actin (Pospich et al., 2020), was topically applied to the slice beginning 3 min post-TBS; slices were harvested 15–18 min later and numbers of densely phalloidin-labeled puncta in CA1 SR field of afferent activation were quantified from epifluorescence images (Fig. 1*c*,*d*) using automated systems described elsewhere (Rex et al., 2007, 2010); prior double-labeling studies demonstrated that these puncta are indeed spines frequently associated with more faintly phalloidin-labeled dendritic processes (Rex et al., 2007). TBS robustly increased the number of densely phalloidin-labeled spines in vehicle-treated slices, and this effect was completely blocked by the competitive NMDAR antagonist APV (100 μM). Remarkably, 30 μM MK-801, the dose that eliminated LTP, did not attenuate the TBS-induced F-actin increase (Fig. 1*d*), thereby indicating that activity-induced actin polymerization requires NMDARs but not the transmembrane ion flux mediated by those receptors. These results constitute evidence that naturalistic patterns of afferent activity initiate actin regulatory, ion flux-independent NMDAR signaling in adult synapses and describe a surprising instance in which a late-stage LTP stabilization event (actin polymerization) occurs in the absence of synaptic potentiation.

Next, we tested the MK-801 sensitivity of TBS-induced increases in phosphorylation of three NMDAR-regulated kinases that play important roles in actin management and LTP. Slices were harvested within 15 min of TBS of the SC system and processed for immunofluorescence analysis of phosphorylated (p) ERK1/2 (T202/Y204), pSrc (Y419), or pCaMKII (T286/T287) colocalized with the postsynaptic excitatory synapse marker PSD95 in the CA1 field of SC afferent activation. Fluorescence deconvolution tomography (FDT) was used to generate 3-D reconstructions of digital image *z*-stacks collected from CA1b SR and to quantify immunolabeled profiles that fell within the size constraints of synapses (Rex et al., 2009; Seese et al., 2013). The density of immunolabeling for the target phosphorylated protein at each double-labeled profile was measured and the resultant values were used to construct fluorescence intensity frequency distributions representing the ~30 thousand synapses per *z*-stack; thus, measures were collected from 80,000 to 120,000 synapses per slice. Consistent with earlier studies (W. Wang et al., 2018a), TBS caused a rightward skew of the intensity frequency distribution, toward greater labeling densities, for synaptic pERK in slices treated with vehicle and MK-801 did not attenuate this effect: the TBS + MK-801 curve was nearly superimposed with the TBS + vehicle curve (Fig. 1*e*). In agreement with previous reports (Chen et al., 2010b; W. Wang et al., 2018a), TBS similarly elevated synaptic pSrc immunoreactivity, and this effect was blocked by APV. But, as with pERK, the TBS-induced increase in synaptic pSrc was unaffected by MK-801 (Fig. 1*f*). MK-801 did, however, block TBS-induced increases in synaptic pCaMKII (Fig. 1*g*). CaMKII is a calcium-dependent kinase that enables activity-driven transfer of AMPA receptors (AMPARs) into synapses and is critical for LTP expression in both sexes (Lisman et al., 2012; Jain et al., 2019; Tullis and Bayer, 2023).

An antagonist of GluN2B blocks TBS-induced LTP in males but not females

The long cytoplasmic tail domain (CTD) of the NMDAR GluN2B subunit plays an important role in NMDAR signaling, synaptic plasticity and memory (Foster et al., 2010; Kessels et al., 2013; Ryan et al., 2013). Recent studies have also implicated GluN2B in ion flux-independent NMDAR functions (Kessels et al., 2013; Y. Li et al., 2022) and in regulation of the subsynaptic actin cytoskeleton (Akashi et al., 2009) although other work indicates that GluN2 subunits are not critical for metabotropic functions that subserve LTD (Wong and Gray, 2018). We used the selective GluN2B-negative allosteric modulator Ro25-6981 (Ro25; Fischer et al., 1997; Karakas et al., 2011) to assess the involvement of this subunit in field CA1 LTP and TBS-induced increases in F-actin beginning with slices from adult male rats. First, we tested if Ro25 (3 μM) depressed pharmacologically isolated NMDAR-mediated responses in CA1 field recordings. A cocktail composed of antagonists of AMPARs (DNQX, 20 μM) and $GABA_A$Rs (picrotoxin, 30 μM) eliminated ~90% of the fEPSP. Subsequent infusion of MK-801 confirmed that the residual response was mediated by NMDAR channel activity (Fig. 2*a*). Ro25 did not measurably affect these NMDAR-gated fEPSPs

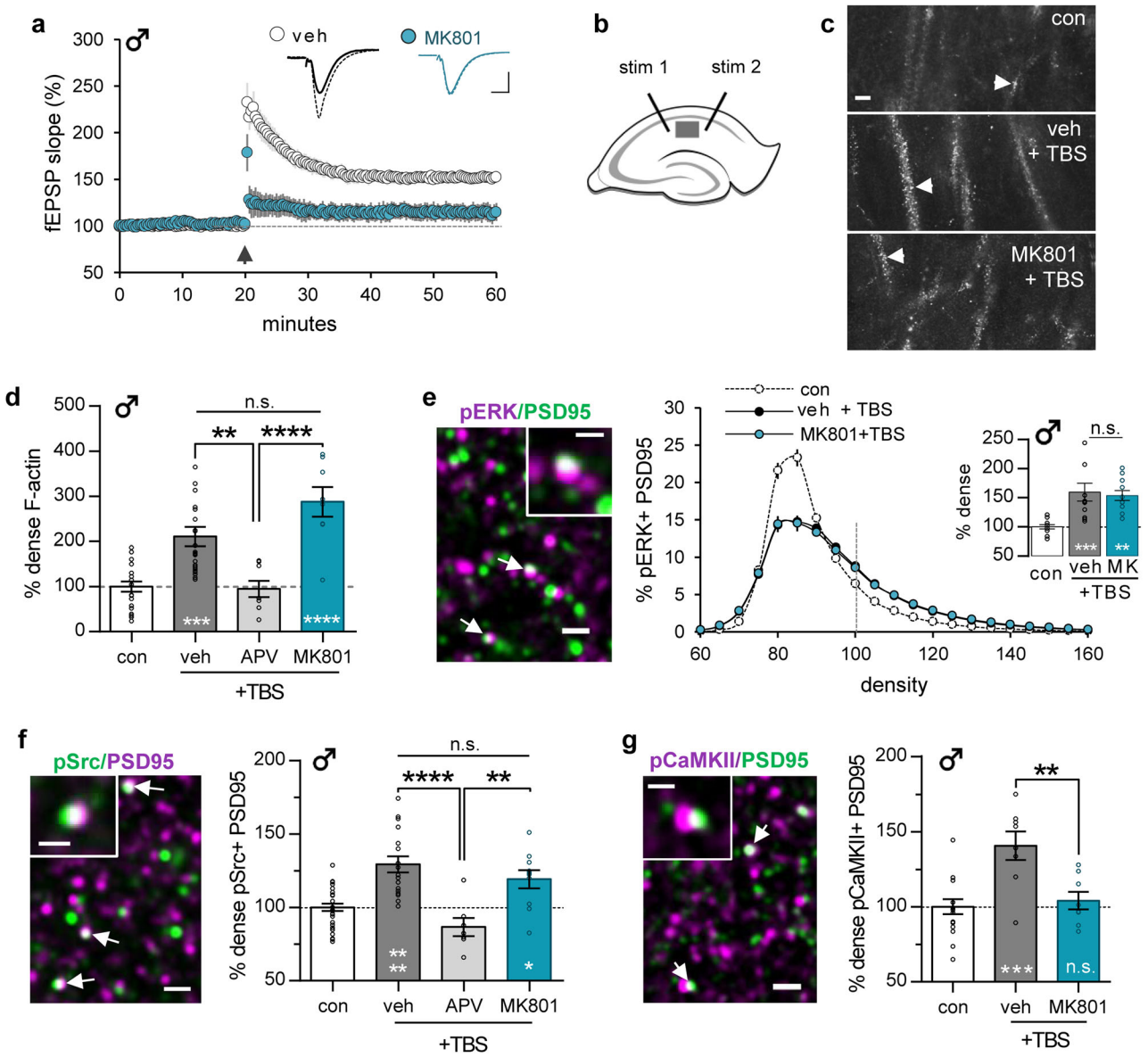

Figure 1. Theta burst stimulation (TBS) elicits nonionotropic NMDAR signaling and actin polymerization. Stimulation was applied to Schaffer-commissural (SC) projections to CA1 str. radiatum (SR) in slices from adult male rats. ***a***, A 10-burst TBS train (arrow) elicited robust CA1 short- and long- term potentiation (STP and LTP, respectively) in vehicle (veh)-treated slices whereas MK-801 (30 μM, introduced 2 h before TBS) blocked this effect ($p = 0.004$ and $p = 0.005$ for STP and LTP, respectively; veh $N = 8$, MK-801 $N = 5$): Traces from before (solid) and 40 min after (dashed) TBS. ***b***, Schematic showing placement of stimulating electrodes in CA1a (stim 1) and CA1c (stim 2); Gray box marks the CA1 SR field of F-actin and signaling protein analysis. ***c***, Images show phalloidin labeling of F-actin (i.e., faint labeling of dendrites decorated with brighter punctate labeling of dendritic spines, arrows) in slices receiving low-frequency control (con) stimulation or TBS in the presence of veh or MK-801 (30 μM). ***d***, Plot shows that TBS increased the proportion of phalloidin-positive puncta that were densely labeled normalized to control slice values ($F_{(3,57)} = 15.30$, $p < 0.0001$; post hoc $p = 0.0001$); this effect was blocked by 100 μM APV (veh vs APV post hoc $p = 0.0046$) but not MK-801 (veh vs MK-801 $p = 0.102$, $N = 8–24$). ***e–g***, Fluorescence deconvolution tomography was used to assess NMDAR contributions to TBS-induced synaptic signaling. Deconvolved images show immunolabeling for the kinase of interest and PSD95; the colors in the heading indicate the fluorophore for each protein; arrows indicate representative puncta with areas of double labeling that appear white (one element with double labeling is shown at higher magnification in an inset). ***e***, TBS caused a rightward skew (toward greater densities) in the density–frequency histogram for synaptic pERK (i.e., colocalized with PSD95; $F_{(38,608)} = 18.50$, $p < 0.0001$; con vs TBS post hoc: $p = 0.0048$); this was unaffected by MK-801. Inset, mean numbers of densely pERK-IR spines (≥100 density units) normalized to control slice values ($F_{(2,32)} = 10.33$, $p = 0.0003$; $N = 11–12$/group) show that TBS increased pERK enriched postsynaptic elements in both veh-treated ($p = 0.0007$) and MK-801-treated ($p = 0.0026$) slices. ***f***, TBS-induced increases of the proportion of synapses with dense pSrc immunoreactivity was blocked by APV (100 μM) but not MK-801 ($F_{(3,62} = 15.11$, $p < 0.0001$; veh vs MK-801 $p = 0.4762$; $N = 7–32$/group). ***g***, TBS increased synaptic pCaMKII, and this effect was blocked by MK-801 ($F_{(2,29)} = 10.53$, $p = 0.0004$; $N = 8–16$/group). Calibration: ***a***, 1 mV, 10 ms; ***c***, 5 μm; ***e–g***, 2 μm; inset, 1 μm. Statistics: ***a***, two-tailed unpaired *t* test; ***e***, two-way repeated-measures ANOVA (interaction) with Bonferroni's post hoc tests (***d***, ***e*** inset, ***f***, ***g***) and one-way ANOVA with Tukey post hoc tests. Asterisks inside bars denote significance versus con stimulation. Asterisks above bars denote significance between TBS groups. n.s., not significant, $*p < 0.05$, $**p < 0.01$, $***p < 0.001$, $****p < 0.0001$. Mean ± SEM values shown. See Extended Data Figure 1-1 for detailed statistics.

(Fig. 2*b*) in agreement with reported effects in slices from adult mice (Hanson et al., 2013). However, Ro25 did reduce NMDAR-mediated EPSCs by ~25% in clamp recordings (Fig. 2*c*). The clamp effect agrees with earlier work that also established an exclusively synaptic location of GluN2B in CA1 (Miwa et al., 2008). The discrepancy between the extracellular versus whole-cell recording results likely reflects the pronounced difference in membrane depolarization generated in the two approaches and thus the degree to which the NMDAR's voltage-sensitive magnesium block is reduced. The results also accord

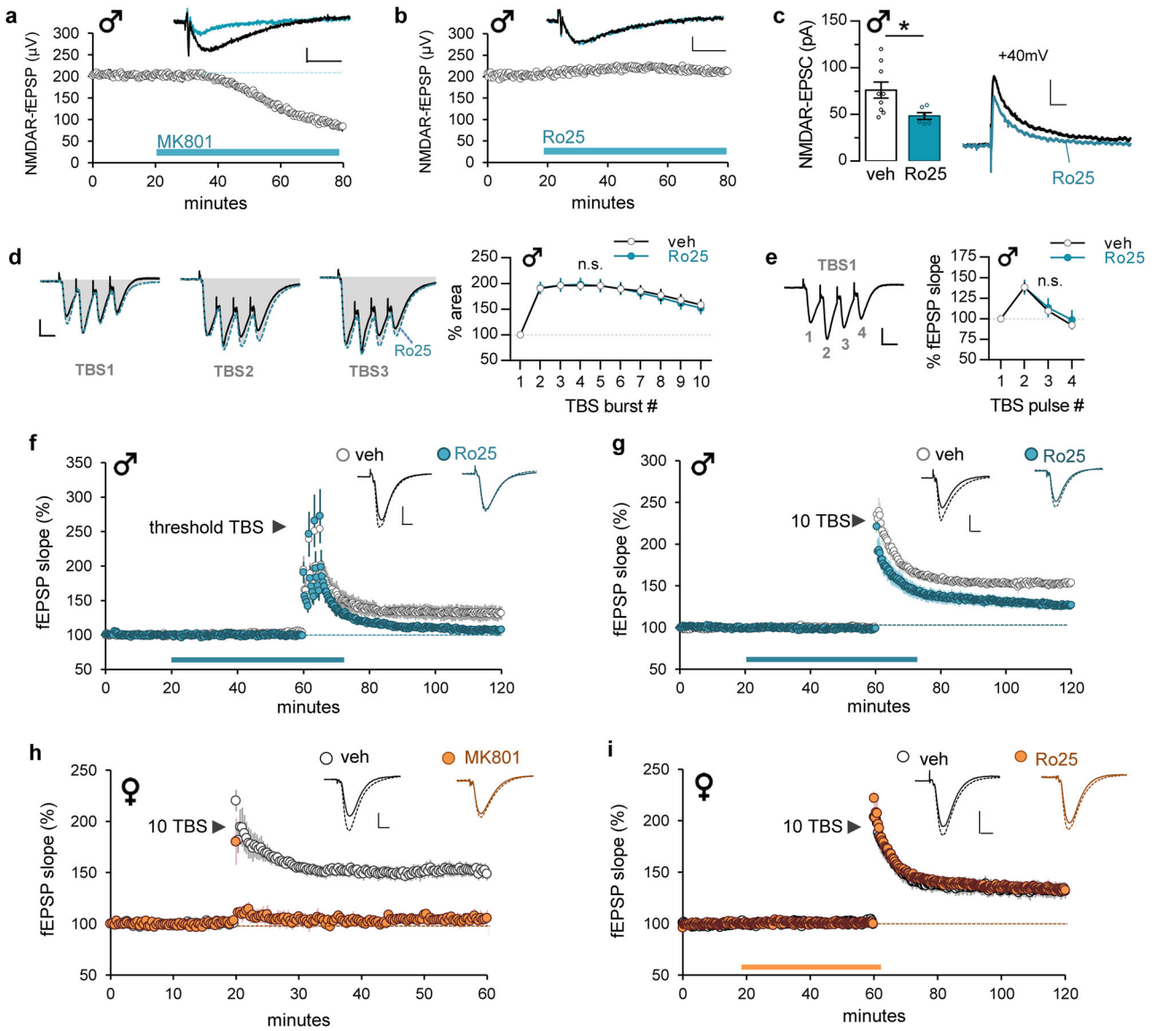

Figure 2. GluN2B-negative allosteric modulator Ro25-6981 (Ro25) blocks SC LTP in males but not females. ***a***, ***b***, In slices from male rats, the isolated NMDAR fEPSP response (i.e., 20 μM DNQX and 30 μM picrotoxin in bath) (***a***) was depressed by MK-801 (30 μM; $N = 6$) but (***b***) not by Ro25 (3 μM; $N = 5$). ***c***, Voltage-clamp recordings from adult male mouse CA1 pyramidal cells held at +40 mV show that Ro25 infusion decreased NMDAR-EPSC amplitude (*$p = 0.0313$; veh $N = 9$, Ro25 $N = 6$). ***d***, In adult male slices, TBS was applied to SC projections and CA1 fEPSP responses were evaluated 40 min after onset of vehicle (veh) or 3 μM Ro25 infusion. Traces at left show responses to the first three bursts in a 10-burst train (veh, black line; Ro25, dashed blue line; burst response area shaded gray). Graph shows that the area of individual burst responses (normalized to first burst) is not altered by Ro25 across the full theta train ($F_{(9,126)} = 0.268$, $p = 0.982$. $N = 7$ veh, $N = 9$ Ro25). ***e***, Measures within first TBS response (i.e., slope size of responses to pulses 2–4 normalized to that of pulse 1) show that the individual response profile was not affected by Ro25 ($F_{(3,42} = 0.189$, $p = 0.903$). ***f***, ***g***, In male rat slices, Ro25 (infused at horizontal bar) significantly reduced SC→CA1 LTP induced by (***f***) threshold-level TBS (4 TBS triplets, spaced by 90 s; $p = 0.008$; $N = 5$/group) or (***g***) a 10-burst TBS train ($p = 0.0015$, veh $N = 7$, Ro25 $N = 9$). ***h***, ***i***, In slices from adult female rats, TBS-induced SC LTP was fully blocked by 30 μM MK-801 (***h***; $p = 0.0008$; veh $N = 5$, MK-801 $N = 4$) but not by Ro25 (***i***; $p = 0.972$; veh $N = 5$, Ro25 $N = 6$). Traces in panels ***f–i*** are from before (solid) and 60 min after (dashed) TBS. Calibration: ***a***, ***b***, 100μV, 20 ms; ***c***, 50pA, 50 ms; ***d–i***, 1 mV, 10 ms. Statistics: two-tailed paired *t* test (***a***, ***b***), unpaired Mann–Whitney *U* test (***c***, ***f***), two-way repeated-measures ANOVA (***d***, ***e***) and unpaired *t* test (***g–i***). Mean ± SEM values shown. See Extended Data Figure 1-1 for detailed statistics.

with suggestions that GluN2B di-heteromeric receptors—the presumed targets for Ro25—are present at low levels in CA1 synapses relative to GluN2A di-heteromers and tri-heteromers (Rauner and Köhr, 2011).

Ro25 had minimal effect on responses to TBS used to induce LTP. With TBS applied 40 min after onset of Ro25 infusion, the area of the individual SC burst responses were comparable through a full 10-burst train ($p = 0.982$; Fig. 2*d*). Moreover, the individual burst response profile, with a peak at pulse 2 and decline from pulses 2 to 4, was comparable in vehicle- and Ro25-treated slices ($p = 0.903$; Fig. 2*e*). These results are pertinent to potential effects of Ro25 on NMDAR-mediated drive to GABAergic interneurons in CA1 SR observed in slices from adult mice (Hanson et al., 2013). Antagonism of GABAergic transmission is known to block the decline in SC response amplitude from pulse 2 to 4 within the burst and to substantially increase in the overall burst response area (Le et al., 2022b). We did not observe either effect with Ro25 treatment of slices from adult male rats.

Despite the minimal effects of Ro25 on NMDAR-mediated fEPSPs and theta burst responses, in adult male slices Ro25 fully blocked LTP that was induced by near-threshold levels of TBS (i.e., 4 theta burst triplets spaced by 90 s; W. Wang et al.,

2018a): The initial STP (i.e., within the first minute post-TBS) was not significantly affected by Ro25 but fEPSP responses returned to baseline levels over an hour ($p = 0.0079$, veh vs Ro25; Fig. 2*f*). Ro25 also significantly reduced LTP that was induced using a full 10-burst theta train (Fig. 2*g*) and, again without effects on STP ($p = 0.0015$ for LTP, $p = 0.066$ for STP; see Extended Data Fig. 1-1 for details on statistics). In agreement with an absence of Ro25 effects on NMDAR-mediated fEPSPs (Fig. 2*b*), the drug did not influence within-train facilitation of burst responses during TBS (Fig. 2*d*).

We then tested effects of MK-801 and Ro25 on LTP in hippocampal slices from adult females. Consistent with the findings in male, MK-801 fully blocked otherwise robust 10-burst TBS-induced STP ($p = 0.0019$) and LTP ($p = 0.0008$) in females (Fig. 2*h*). However, in striking contrast to effects in males, Ro25 did not measurably dampen the magnitude of either STP ($p = 0.529$) or LTP ($p = 0.972$; Fig. 2*i*), thereby demonstrating marked sex differences in the involvement of GluN2B in SC→CA1 potentiation.

Sex differences in receptors critical for TBS-induced actin polymerization

Next, we used Ro25 to test if GluN2B is critical for activity-induced actin remodeling. In slices from adult male rats, infusion of Ro25 completely blocked TBS-induced increases in phalloidin-labeled spine F-actin (Fig. 3*a*), consistent with the

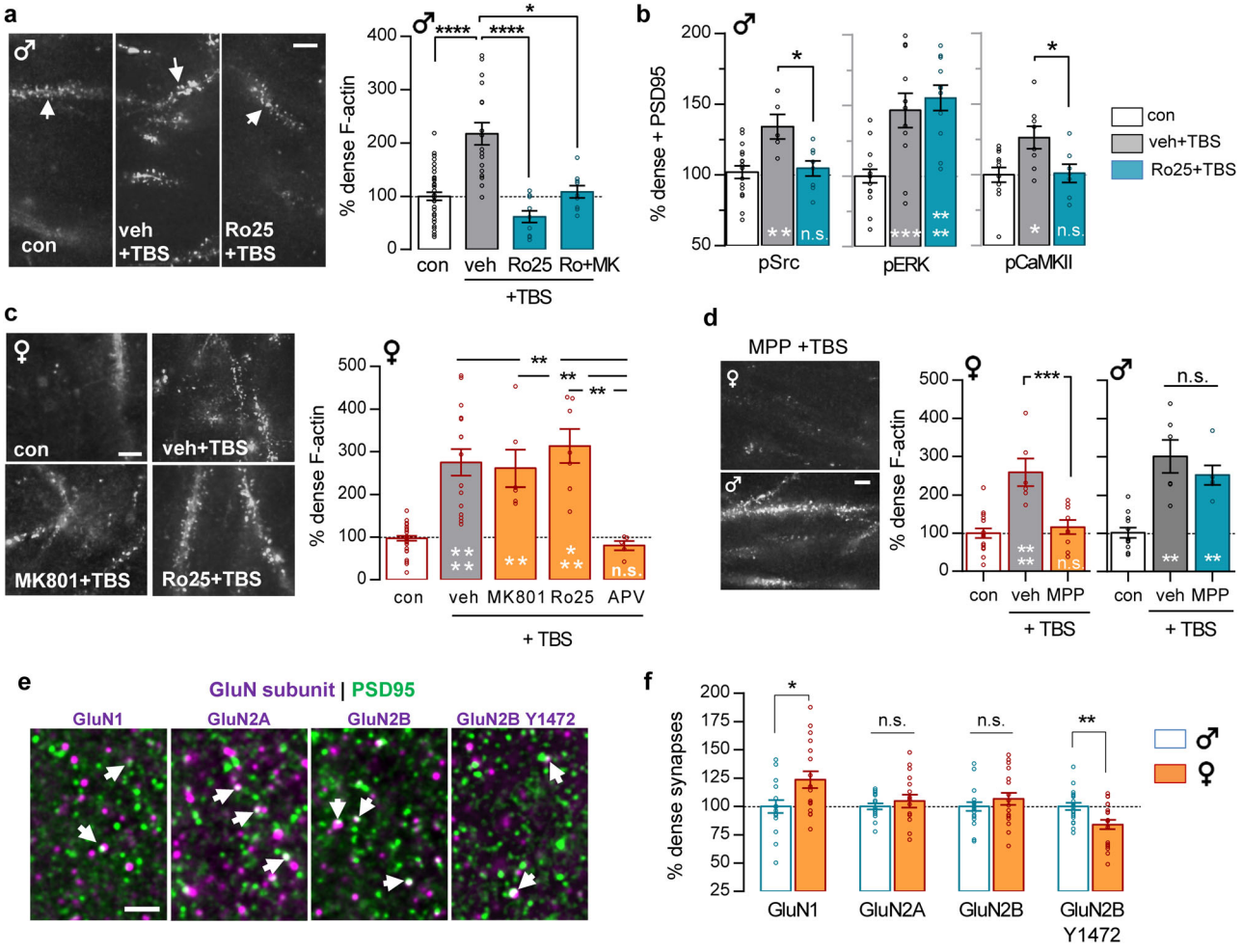

Figure 3. GluN2B-negative allosteric modulator Ro25-6981 (Ro25) blocks TBS-induced increases in spine F-actin in males but not females. Hippocampal slices received either control (con) low-frequency stimulation or 10 TBS of Schaffer-commissural (SC) afferents to CA1 in the presence of MK801 (30 μM) or Ro25 (3 μM), and then phalloidin labeling of F-actin or synaptic protein levels were evaluated in CA1 SR (blue and orange bars denote results from males and females, respectively). ***a***, In males, TBS doubled the proportion of spines with dense phalloidin labeled F-actin in vehicle (veh)-treated slices and this effect was completely blocked by Ro25 applied alone (post hoc $^{****}p < 0.0001$) or in the presence of MK-801 ($^{*}p = 0.0304$, $N = 9$–40/group; points denote individual slice measures). In ***a–d***, bar graphs indicate values normalized to con mean; images show phalloidin labeling in CA1 SR in representative cases. ***b***, In males, Ro25 blocked the TBS-induced increase in the proportion of PSD95-IR synapses with dense immunolabeling for pSrc and pCaMKII but not that for pERK (pSrc: $F_{(2,27)} = 6.517$, $p = 0.0049$; $N = 5$–17/group; pERK, $F_{(2,36)} = 14.36$; $p < 0.0001$, $N = 11$–17/group; pCaMKII: $F_{(2,24)} = 5.111$, $p = 0.0142$; $N = 7$–12/group). ***c***, In slices from females, TBS elicited comparable increases in punctate phalloidin labeled F-actin in the presence of veh, MK-801, and Ro25, but this effect was blocked by NMDAR antagonist APV ($p < 0.0001$; $N = 5$–33). ***d***, TBS-induced increased numbers of densely phalloidin labeled puncta in CA1 SR are blocked by ERα antagonist MPP (3 μM) in females ($F_{(2,29)} = 16.02$, $p < 0.0001$; $N = 6$–17) but not in males ($p = 0.0003$; $N = 6$–12). ***e***, Deconvolved images show dual immunolabeling for NMDAR subunits (magenta) and PSD95 (green) in CA1 SR; arrows indicate double-labeled profiles. ***f***, Quantification of immunofluorescence intensity (for puncta double-labeled for PSD95; female values normalized to male mean) shows that the proportion of postsynaptic elements with dense GluN1-immunoreactivity was greater in females than that in males ($p = 0.0171$) whereas levels of GluN2A- and GluN2B-immunoreactivity were comparable ($N = 17$–20/group). The proportion of PSD95-IR elements with dense pGluN2B Y1472 immunoreactivity was lower in females than that in males ($p = 0.0041$; $N = 17$–20/group). Scale bars: ***a***, ***c***, ***d***, 5 μm; ***e***, 2 μm. Statistics: ***a***, ***c***, ***d***, male, Kruskal–Wallis with Dunn post hoc; ***b***, ***d***, female, one-way ANOVA with Tukey's post hoc; ***f***, two-tailed unpaired *t* test excepting NR2A (Welch's correction). Asterisks inside bars denote comparison with controls; n.s., not significant, $^{*}p < 0.05$, $^{**}p < 0.01$, $^{***}p < 0.001$, $^{****}p < 0.00001$. Mean ± SEM values shown. See Extended Data Figure 1-1 for detailed statistics.

drug's actions on LTP consolidation in males. Ro25 also eliminated TBS effects on pSrc colocalized with PSD95 at CA1 synapses but did not attenuate the pERK response (Fig. 3*b*). GluN2A-containing NMDARs are known to upregulate ERK phosphorylation (Sun et al., 2018) independent of calcium (L. J. Li et al., 2016); this, together with contributions of TrkB signaling (Scharfman and MacLusky, 2006), might explain the pERK result. Finally, in males Ro25 blocked TBS-induced increases in synaptic pCaMKII immunoreactivity, indicating that in males both ionotropic and nonionotropic NMDAR functions are needed to engage this LTP-critical protein.

In hippocampal slices from adult females, TBS-induced increases in spine F-actin were totally blocked by APV but unaffected by MK-801 infusion (Fig. 3*c*); these reagents had the same effects in male slices (Fig. 1*d*), thereby indicating that, in both sexes, activity-induced actin polymerization relies on the NMDARs but not on ion flux mediated by those receptors. However, in marked contrast to effects in males, Ro25 did not block or dampen TBS-induced increases in spine F-actin in females (Fig. 3*c*), a result consistent with the lack of Ro25 effect on female SC LTP. Recent work has shown that in female, but not male, field CA1, locally derived estrogen acting through membrane estrogen receptor alpha (ERα) is critical for LTP and TBS-driven activation of various kinases upstream from F-actin assembly (Vierk et al., 2012; W. Wang et al., 2018a; Gall et al., 2024). In accord with this, infusion of the ERα antagonist MPP (3 μM) prevented TBS-induced increases in spine F-actin in females but not in males (Fig. 3*d*). This result suggests that in CA1 pyramidal cells, females substitute local estrogen signaling through ERα for ion flux-independent NMDAR operations present in males for the rapid activity-induced remodeling of actin networks in mature spines.

The failure of Ro25 to disrupt TBS-induced increases in F-actin and LTP in females raises the possibility that there are sex differences in concentrations or post-translational modifications of synaptic GluN2B subunits. To assess the first of these possibilities, FDT was used to measure levels of immunoreactivity for NMDAR subunits GluN1, GluN2A, and GluN2B colocalized with PSD95 in CA1b SR. These measures detected a modest sex difference in postsynaptic concentrations of GluN1 but comparable levels of GluN2A and GluN2B (Fig. 3*e*,*f*). However, levels of pGluN2B Y1472 (Shipton and Paulsen, 2014) were significantly lower in females than those in males ($p = 0.0041$, two-tailed unpaired t test), suggesting a modification that could diminish the contributions of GluN2B to actin regulation and LTP stabilization in females.

Sex differences in metabotropic receptors underlying memory

Episodic memory depends on the hippocampus and the integrity of LTP in hippocampal pathways (B. M. Cox et al., 2019; Amani et al., 2021; Chavez et al., 2022). Although evidence for the specific involvement of field CA1 is limited, the CA1 pyramidal cells exhibit distinct firing patterns during nonspatial odor sequence learning in rat (Gattas et al., 2022), and studies in human have shown episodic memory relies on the integrity of CA1 (Bartsch et al., 2011). In this context, the aggregate SC LTP results described above give rise to the predictions that blocking GluN2B-mediated m-NMDAR functions will more severely impair episodic learning in males than that in females and, conversely, that blocking ERα will disrupt this learning in females but not that in males. We tested this by treating mice with vehicle, GluN2B antagonist Ro25 (5 mg/kg, 30 min), or ERα antagonist MPP (0.6 mg/kg, 60 min) prior to initial odor exposure in the 4-odor "Where" task (B. M. Cox et al., 2019; Brunetti et al., 2024). In this paradigm, mice are exposed to four simultaneously presented odors for 10 min, and, at testing 24 h later, they are exposed to the same odors but with the positions of two having been switched (Fig. 4*a*). Vehicle-treated mice of both sexes preferentially explored the familiar odors in novel locations indicating that they had acquired information on their original positions (Fig. 4*b*,*c*). Treatment with Ro25 prior to the initial odor exposure blocked discrimination of novel location odors in males without effect in females (Fig. 4*b*), indicating GluN2B was critical for the acquisition of location information in males only. Conversely, in this same task, MPP eliminated discrimination of the novel location odors in females without effect on performance in males (Fig. 4*c*). Neither Ro25 nor MPP influenced total cue sampling times or locomotor activity (distance and velocity of travel) in either sex (Fig. 4*d*–*g*), indicating that the compounds did not have reliable effects on arousal or interest in the cues. These results suggest that males and females rely upon nonionotropic signaling from different types of receptors for encoding the spatial component of episodic memory.

Sex differences in episodic learning

Given evidence for sex differences in receptors involved in episodic "Where" encoding described above, we tested if males and females differ in their ability to acquire information on three major features of an episode including the identity, location, and sequence of events or items encountered (i.e., What, Where, and When information; Tulving, 1984; Dere et al., 2005b; Eacott and Easton, 2010). Episodic encoding occurs without rehearsal or reinforcement and always has a temporal dimension which has been proposed to be the principal organizer of the encoded information (Ekstrom and Ranganath, 2018; Umbach et al., 2020); in these and other ways, it is distinct from simple object recognition and operant learning typically used in animal experiments (Tulving, 1984). Thus, the paradigms used here involved exposure to multiple cues and did not include practice or reward (W. Wang et al., 2018b; B. M. Cox et al., 2019). To test "What" (cue identity) acquisition, mice were exposed to a sequence of three different odor pairs (A > B > C), followed by a retention trial that paired a previously exposed odor with a novel odor (A vs D; Fig. 5*a*). As rodents preferentially investigate novel stimuli (Berlyne, 1950; Dere et al., 2005b), more time spent exploring the novel versus the previously sampled cue indicates that the latter was remembered. Both sexes preferentially explored the novel odor and had similar DIs (40.9 ± 7.2 and 41.8 ± 7.8, for males and females, respectively; $p = 0.94$, unpaired t test; Fig. 5*a*). However, when presented with four odor pairs in sequence, females later discriminated the novel cue but males did not (male vs female DI: 7.3 ± 4.2 vs 35.3 ± 4.5; $p = 0.0003$; Fig. 5*a*). We reevaluated performance in an alternative episodic "What" task in which mice were allowed to freely investigate four different odors presented together in the same 5 min session (A-B-C-D; placed in fixed arena positions). At testing 48 h later, one of the cues was replaced with a novel odor. Females discriminated and preferentially explored the novel odor, but males did not (Fig. 5*b*).

Next, we tested acquisition of the temporal order of cue presentation (episodic "When"). Previous studies showed that male mice exposed to a series of four consecutive odor pairs (A > B > C > D) spend more time investigating the less recent odor B versus more recent odor C in subsequent retention testing (B. M. Cox et al., 2019). The same result was obtained when the initial odor presentations were separated by 30 s or 5 min, suggesting that mice acquire information about the order of cue

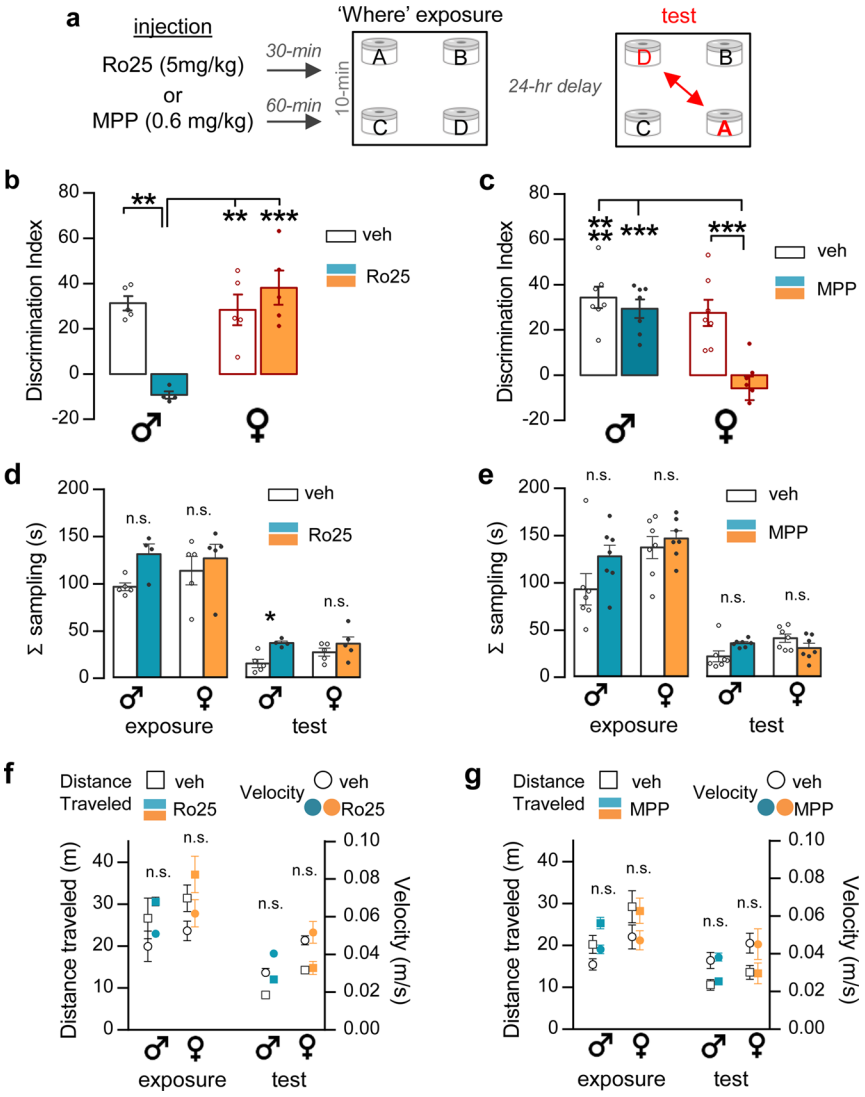

Figure 4. Sex differences in the effects of GluN2B and ERα antagonists on episodic "Where" encoding. ***a***, Mice received vehicle, Ro25, or MPP treatment before odor exposure in the four-corner episodic "Where" paradigm illustrated. ***b***, ***c***, Vehicle (veh)-treated males (blue) and females (orange; separate cohorts in panels ***b*** and ***c***) preferentially sampled the cues moved to novel locations. ***b***, Ro25 blocked discrimination of novel location cues in males ($F_{(1,15)} = 19.62$, $p = 0.0005$; veh $N = 5$, Ro25 $N = 4$) but had no effect on female performance ($N = 5$/group). ***c***, ERα antagonist MPP fully blocked discrimination of the moved cues in females but did not affect performance in males ($F_{(1,24)} = 8.001$, $p = 0.0093$; $N = 7$/group). ***d–g***, Measures of total (Σ) cue sampling times in seconds (***d***, ***e***) and locomotor activity (distance traveled and velocity) (***f***, ***g***) during both initial cue exposure and testing were not influenced by treatment (MPP, Ro25) in males or females (interaction, $p > 0.05$). Statistics: two-way ANOVA with post hoc Tukey. n.s., not significant, *$p < 0.05$, **$p < 0.01$, ***$p < 0.001$, ****$p < 0.0001$. Mean ± SEM values shown. See Extended Data Figure 1-1 for detailed statistics.

presentation as opposed to the time since last exposure. Here, we used the same initial exposure to a sequence of four identical odor pairs but, in the retention trial, placed a heavier demand on memory by presenting together the temporally more distant cues A versus B. In contrast to results for the B versus C comparison, males had no evident preference for A versus B, whereas females preferentially explored A over B and thus had higher DIs than males in the same cohort (Fig. 5*c*).

Finally, we tested spatial encoding (episodic "Where") by allowing mice to sample four simultaneously presented odors for 5 min and then tested 5 min later to determine if they discriminated, and preferentially sampled, two cues that were swapped to assume novel positions (the positions of cues were fixed in exposure and training trials). Under these conditions with a shorter period of initial cue exposure and shorter delay from initial sampling to testing, relative to the drug studies described above, males preferentially explored the switched (novel location) odors but females did not (Fig. 5*d*).

Importantly, for all behavioral studies there were no systematic, cross-paradigm sex differences in the total time spent sampling cues during initial exposure or retention trials (Figs. 4*d*,*e*, 5*f*,*h*,*j*,*l*,*n*). Similarly, travel distance and velocity were comparable between sexes (Figs. 4*f*,*g*, 5*g*,*i*,*k*,*m*,*o*).

We summarized the results for the four episodic memory tests by expressing retention for each female mouse as a *z*-score difference from the mean DI of the male group. This provided a relative estimate for female versus male performance in each assay. The main effect of sex was highly significant ($F_{(3,21)} = 49.11$; $p < 0.0001$). The strongest female performance was evident in the simultaneous "What" test ($p < 0.015$ vs other tests) although females also had higher DI scores than males in the serial four-odor "What" and "When" tests. Scores for females were

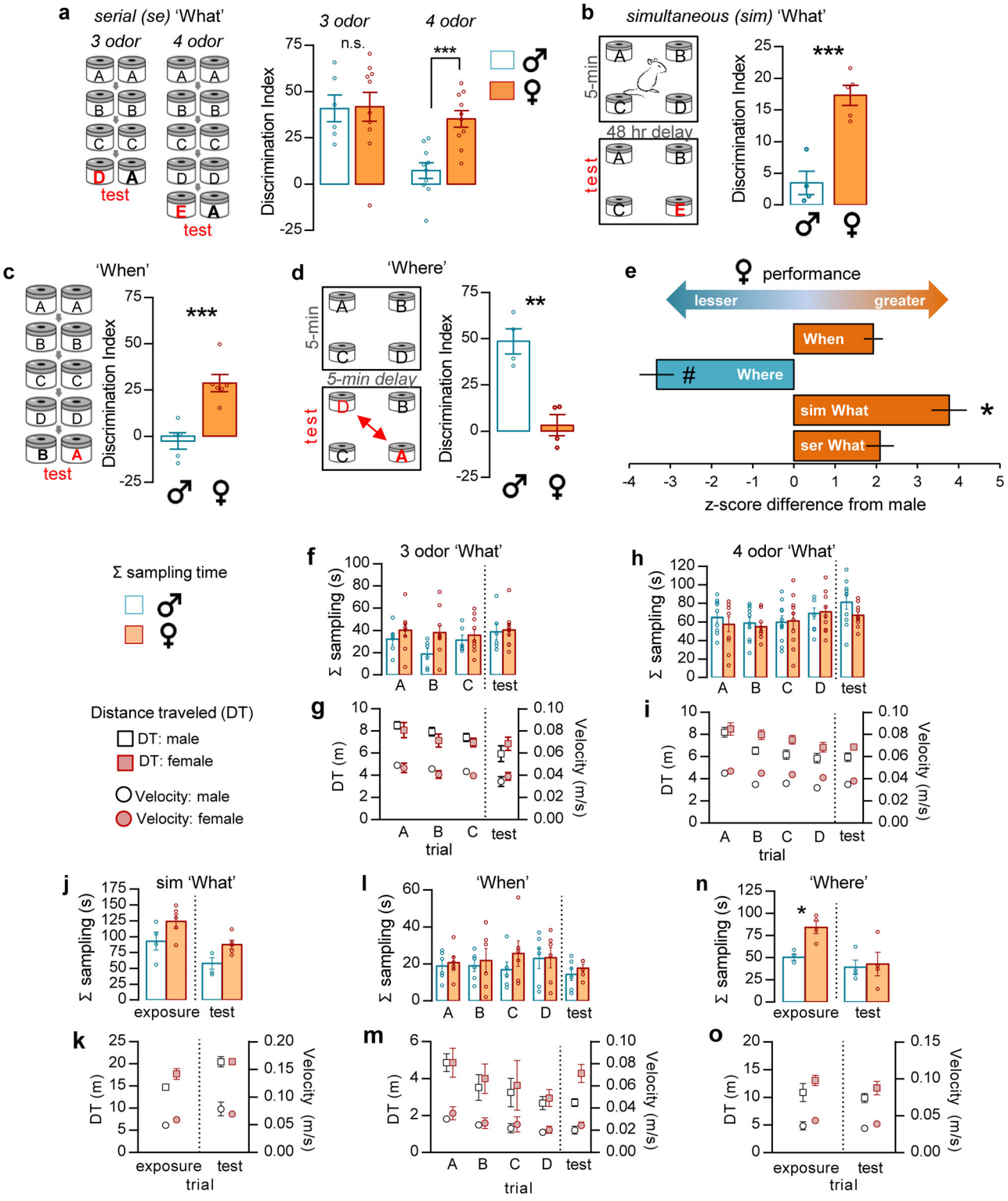

Figure 5. Sex differences in the acquisition of the What, When, and Where components of episodic memory. ***a***, Left, Schematic of the serial odor "What" task using initial exposure (black) to three and four odors in series; in this and other schematics the novel cue or cue in novel location is indicated in red. Right: Bar graphs show that, in the three-odor task, both males (blue) and females (orange) preferentially explored the novel (D) versus the familiar (A) odor at testing ($p = 0.94$; male $N = 6$, female $N = 10$), whereas with initial exposure to a series of four odors, females preferentially explored the novel odor at testing but males did not ($p = 0.0003$; male vs female, $N = 10$/group). ***b***, Left, Schematic of the Simultaneous "What" task. Right, At testing, females distinguished the novel from previously experienced odors but males did not ($p = 0.0007$; male $N = 4$ vs female $N = 5$). ***c***, Left, Schematic of the "When" task. Right, Females preferentially sampled the least recently exposed odor but males did not ($p = 0.001$; male $N = 5$, female $N = 6$). ***d***, Left, Simultaneous "Where" task schematic. Right, At testing males preferentially explored the novel location odors but females did not ($p = 0.0022$, $N = 4$/group). ***e***, Female performance in the What, When, and Where tasks expressed as a *z*-score difference from the male group discrimination index mean. The female performance in the Simultaneous (sim) "What" task was greater than for the other tasks ($F_{(3,21)} = 49.11$, $p < 0.0001$; post hoc $^*p \leq 0.15$; $N = 4$–10/group) and results on the "Where" tasks differed from the other three scores (# $p < 0.0001$). ***f–o***, Top bar graphs show group means of total (Σ) sampling times in the initial exposure trial(s) leading to the test trial in a particular memory task. Bottom plots show the total distance traveled (DT, squares) and movement velocity (circles) during the same sessions. Analysis of interaction (sex*trial) via two-way ANOVA revealed no significant difference in the total time spent sampling odors during initial exposure and test trials for both serial

markedly lower than those for males in the "Where" test only ($p < 0.0001$ vs other tests; Fig. 5*e*). It is noteworthy that the same initial cue exposure trial used in the simultaneous "What" and "Where" tasks yielded the greatest sex differences depending on which aspect of learning—cue identity versus spatial location—was tested.

Discussion

As with memory, LTP passes through multiple consolidation stages during which it is vulnerable to disruption by diverse manipulations (Larson et al., 1993; Huang and Hsu, 2001; Lynch et al., 2013). As demonstrated for the SC system, processes underlying this stabilization include small GTPase-initiated signaling cascades leading to the formation and subsequent stabilization of actin filaments (Kramár et al., 2006; Rex et al., 2009; Gall et al., 2021). These events serve to anchor changes to the dendritic spine and postsynaptic specialization (Krucker et al., 2000; Bramham, 2008; Lynch et al., 2013). Results presented here led to the surprising conclusion that this complex collection of events, while dependent upon NMDARs, can be completed without NMDAR-mediated calcium influx. Blocking the NMDAR channel with MK-801 entirely eliminated CA3→CA1 LTP without disrupting actin regulatory signaling and increases in spine F-actin required for stabilization of the potentiated state. The channel blocker thus produced a peculiar condition in which TBS activated processes that support LTP consolidation in the absence of LTP expression. Further experiments showed that GluN2B-dependent, nonionotropic functions of the NMDAR are needed for TBS-induced increases in pSrc and F-actin and for LTP stabilization in males only. In contrast, females relied on ERα rather than GluN2B to trigger actin polymerization and consolidation of the potentiated state (Fig. 6). Sex differences in receptor involvement were also evident in the substrates for episodic memory. Specifically, the GluN2B antagonist Ro25-6981 completely disrupted encoding of the "Where" component of episodic memory in males but had no such effect in females. Conversely, blocking ERα prevented acquisition of "Where" information in females but not males, thereby paralleling its effects on actin signaling and LTP. These results indicate that, in both sexes, the specific metabotropic receptor that supports SC LTP contributes to hippocampus-dependent episodic memory.

The present results are consistent with prior evidence for m-NMDAR contributions to synaptic plasticity in CA1. This was first described for SC LTD (Nabavi et al., 2013; Dore et al., 2016; but see Gray et al., 2016) and then for bidirectional changes in spine size elicited by glutamate uncaging (Stein et al., 2015, 2021). The latter studies demonstrated m-NMDAR-dependent spine expansion in both sexes but tests for GluN2B or ERα involvement were not conducted, and it remains unclear if the sex differences in metabotropic activities described here were present. Nevertheless, the uncaging studies showed that both m-NMDAR signaling and calcium influx are needed for spine enlargement (Stein et al., 2021).

There are multiple steps beyond actin polymerization (Kramár et al., 2006; Chen et al., 2010b), including stabilization of newly formed filaments (Rex et al., 2009, 2010) and recovery of integrin signaling (Babayan et al., 2012), that are needed to complete LTP consolidation. Whether these are also driven by nonionotropic NMDAR signaling is an important issue for future work. Notably, treatment with Ro25-6981 in males or with ERα antagonist MPP in females did not detectably reduce the initial expression of potentiation. Both TBS (Chen et al., 2007) and glutamate uncaging (Bosch et al., 2014) increase the size of postsynaptic densities, a modification that is a likely prelude to expansion of the AMPAR pool and accordingly LTP expression. Given that MK-801 blocks the earliest signs of potentiation (i.e., STP), whereas suppression of metabotropic signaling does not, we conclude that the transient increases in spine calcium required for LTP induction (Lynch et al., 1983; Malenka et al., 1988; Stein et al., 2021) are primarily responsible for synapse expansion. At least two LTP-related effects have been linked to the cation: proteolysis of cytoskeletal anchoring proteins by calcium-dependent proteinases (calpains; Lynch and Baudry, 1984, 2015; Vanderklish et al., 1996; Zhu et al., 2015) and activation of CaMKII (Lisman et al., 2012; Tullis and Bayer, 2023). Proteolysis is thought to relax constraints on spine morphology, a likely prerequisite for shape change, whereas CaMKII is important for both spine expansion (Ueda et al., 2022; Tullis and Bayer, 2023) and AMPAR movement into the synapse (Hayashi et al., 2000). The present studies confirmed an earlier report (C. D. Cox et al., 2014) that TBS activates postsynaptic CaMKII and further demonstrated that this effect is blocked by MK-801. Together, the results point to the conclusion that ionotropic NMDAR operations induce LTP, independent of metabotropic actions, via effects on synapse size and the synaptic AMPAR pool.

The present studies did not identify specific links between GluN2B and actin management but there are several likely possibilities. Src influences postsynaptic actin polymerization in part via Crk-associated substrate (CAS) phosphorylation and consequent influences on Abelson tyrosine kinase which regulates actin polymerization (D. D. Tang and Anfinogenova, 2008; Koleske, 2013). Moreover, the long GluN2B-CTD associates with SynGAP (Sun et al., 2018), which is concentrated at excitatory synapses and there regulates cofilin and thus actin polymerization (Carlisle et al., 2008). SynGAP also potently influences the activity of Rap (Krapivinsky et al., 2004), a GTPase involved in integrin activation (Ortega-Carrion et al., 2016). Integrins regulate the actin cytoskeleton at adhesion junctions throughout the body (Blystone, 2004; Geiger et al., 2023) and are essential for TBS-induced F-actin assembly in hippocampal dendritic spines in both sexes (Kramár et al., 2006). As described, it appears that females substitute local release of estrogen onto ERα (W. Wang et al., 2018a and present results) for GluN2B-dependent actions that are critical for actin polymerization and LTP in males. Thus, we propose that both sexes use a combination of ionotropic and metabotropic operations to modify synapses with LTP but execute the metabotropic functions in markedly different ways (Fig. 6). As this is the first report of sex differences in nonionotropic contributions of the NMDAR to LTP, we do not know the extent to which these sex-specific functions are present in other brain areas. However, a recent study found that potentiation of hippocampal projections to nucleus accumbens is NMDAR dependent in males but relies on ERα

←

"What" tasks (***f***, ***h***), simultaneous "What" (***j***), "When" (***l***), and "Where" (***n***) ($p > 0.05$). ***g***, ***i***, ***k***, ***m***, ***o***, The significance of interaction was also absent in measures of distance traveled and velocity across the same tasks ($p > 0.05$). Statistics: ***a–d***, two-tailed unpaired *t* test; ***e***, one-way ANOVA, post hoc Tukey; ***f–o***, two-way ANOVA; n.s., not significant, $*p < 0.05$, $**p < 0.01$, $***p < 0.001$. Mean ± SEM values shown. See Extended Data Figure 1-1 for detailed statistics.

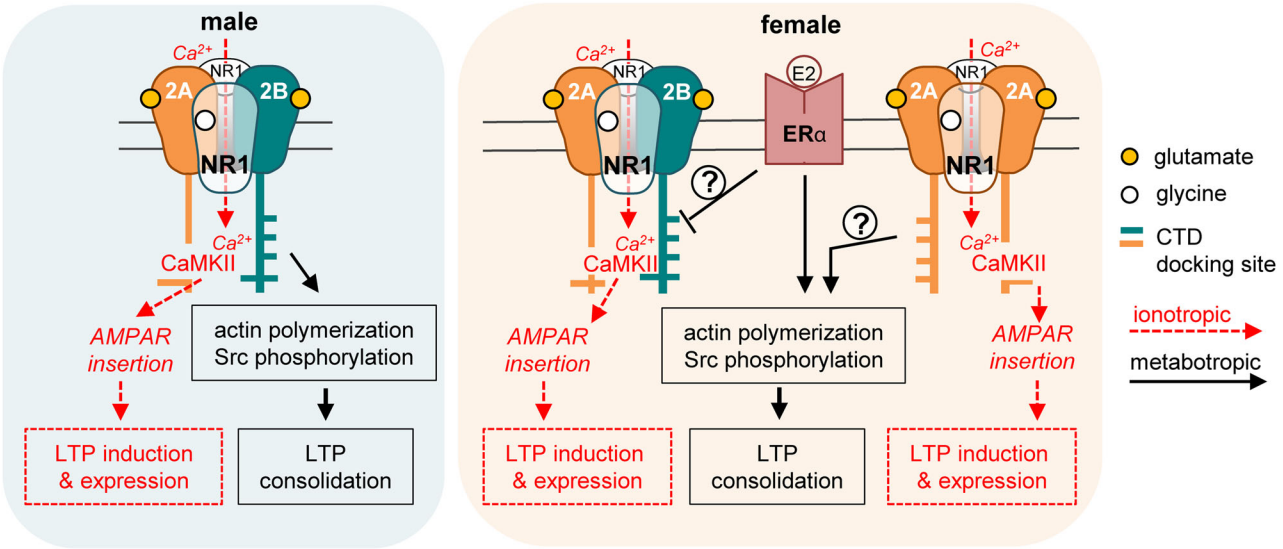

Figure 6. Schematic illustration of mechanisms proposed to underlie sex differences in ion flux-independent NMDAR contributions to memory-related SC LTP. Observed effects of APV and MK-801 indicate that both males and females use ionotropic NMDAR functions to activate CaMKII and associated processes (e.g., AMPAR insertion) required for the induction of field CA1 LTP (indicated in red font). The present results show that both sexes also rely upon nonionotropic NMDAR functions (i.e., those blocked by APV but not by MK-801) for TBS-induced postsynaptic actin polymerization, Src phosphorylation, and LTP. Sex-specific effects of Ro25-6981 described here indicate GluN2B subserves these nonionotropic NMDAR functions in males, presumably via the subunit's cytoplasmic terminal domain (CTD) that acts as a docking site for signaling proteins including Src family kinases, SynGAP and CAMKII. Females do not use the Ro25-sensitive GluN2B mechanism for TBS-induced increases in postsynaptic F-actin or SC LTP but instead rely upon synaptic ERα to engage the same effectors as used by males. We propose that in females estrogen receptor alpha (ERα) may tonically suppress GluN2B activities by reducing phosphorylation of its CTD Y1472 site, thereby modulating CaMKII binding (Tullis and Bayer, 2023). However, results showing that, in females, APV blocks the TBS-induced increase in F-actin whereas MK-801 does not suggests that females do have m-NMDAR contributions to the LTP consolidation machinery; we speculate that the GluN2A CTD may contribute to these functions in females.

and voltage-gated calcium channels in females (Copenhaver and LeGates, 2024).

Synaptic ERα levels in CA1 are higher in females than those in males and estradiol acts through ERα to activate postsynaptic Src and ERK in females only (Wang et al., 2018a). Moreover, protein kinase A (PKA) levels are higher in males and it has been argued that males do not need estrogen-induced increases in PKA activity to suppress phosphatases and thereby enable kinase signaling whereas females do need PKA for both estrogen- and activity-induced SC potentiation (Jain et al., 2019). These findings suggest two reasons why male rodents, despite having high estrogen levels in the hippocampus (Hojo and Kawato, 2018), do not appear to use the endogenous hormone to promote LTP (W. Wang et al., 2018a). Why m-NMDAR activities that support LTP in males are missing in females is not known but we found the synaptic GluN2B Y1472 site is more highly phosphorylated in males. This NMDAR CTD residue is targeted by Src kinases that are known to upregulate NMDAR function (Scanlon et al., 2017; Rajani et al., 2021). Evidence that estrogen decreases GluN2B Y1472 phosphorylation (Waters et al., 2019) raises the possibility that the synaptic estrogen signaling needed for consolidation of female LTP simultaneously suppresses nonionotropic activities of GluN2B-containing NMDARs (Fig. 6). Possibly related to this, it has been reported that GluN2B mediates applied estradiol's effects on LTP in ovariectomized female rats (Smith et al., 2009, 2016; Nebieridze et al., 2012). The extent to which this effect relates to processes described here for gonadally intact females and endogenous estrogen action is uncertain.

Differences in the receptor systems mediating metabotropic signaling underlying spine actin remodeling with LTP were accompanied by striking sex differences in the acquisition of episodic memory: males exhibited better retention of "Where" information whereas females had higher scores on tests for the identity ("What") and temporal sequence ("When") of sampled cues. Importantly, males performed well on "What" and "When" tasks when presented with a shorter list of cues and females had good retention scores on the episodic spatial task when given additional time to explore odor locations. These results indicate that pronounced sex differences in retention emerge as task demands increase. Although the sex differences in learning described here are unprecedented for rodent work, they do have correspondences with results of human studies in which males typically have higher scores in spatial tasks whereas females have better scores in tests for nonspatial components of episodic memory (Barel and Tzischinsky, 2018; Asperholm et al., 2019; Voyer et al., 2021) and retention of extended lists (Youngjohn et al., 1991; Kramer et al., 1997; Rehnman and Herlitz, 2007).

Although our pharmacological results indicate that sex differences in LTP consolidation machinery have consequences for episodic learning, how the synaptic dimorphism might relate to differential encoding of "What," "Where," and "When" information is unclear. Prior work has shown that in females the inclusion of locally derived estrogen (Naftolin et al., 1996; Balthazart et al., 2006; Vierk et al., 2012) into the already complex consolidation machinery results in a higher (relative to males) threshold for producing stable LTP (W. Wang et al., 2018a). There have been no tests for sex differences in the threshold for activating processes that erase recently induced potentiation. Theta frequency stimulation (i.e., trains of single pulses at 5 Hz) can eliminate SC LTP if applied in the first few minutes after induction with TBS (Larson et al., 1993; Huang and Hsu, 2001). Thus, it is possible that activity patterns associated with encoding new information can under some circumstances reduce the strength of traces formed by earlier items in a list. Notably, the weaker performance by males relative to females occurred

in episodic tasks involving serial presentation of cues. It will be of interest to determine if the LTP reversal process is activated with lower threshold in males as compared with females and if this difference impacts the ability to retain information on serial cues. Learning in the episodic "Where" paradigm aligned with the sex differences in SC LTP thresholds in that males required less time than females to encode cue locations. Importantly, and unlike the serial cue "What" and "When" paradigms, there were only brief delays between encounters with the various cues in the spatial task and the mice were able to sample and resample odors in various sequences.

Beyond effects on episodic memory, sex differences in metabotropic receptors that support LTP could contribute to the differential vulnerability of cognitive processes to insults and disease states. As one case in point, we have shown that in female mice, exposure to delta-9-tetrahydrocannabinol during adolescence leads to an enduring loss of estrogen responsiveness by CA1 pyramidal cells (Le et al., 2022a). This was associated with a loss of LTP consolidation and impaired CA1-dependent object location memory in females only. Conversely, disturbances in NMDAR function (Zhou and Sheng, 2013; Mielnik et al., 2021) might have greater impact in males. In animal models of schizophrenia, which is more prevalent in males, symptoms are potentiated by NMDAR antagonism in males and blunted by estrogen treatment (Gogos et al., 2012; Wickens et al., 2018). Together these findings indicate that an appreciation of sex differences in mechanisms of synaptic plasticity may prove critical for the informed design and use of therapeutics (Dong et al., 2023) for cognitive impairments.

References

Akashi K, Kakizaki T, Kamiya H, Fukaya M, Yamasaki M, Abe M, Natsume R, Watanabe M, Sakimura K (2009) NMDA receptor GluN2B (GluR epsilon 2/NR2B) subunit is crucial for channel function, postsynaptic macromolecular organization, and actin cytoskeleton at hippocampal CA3 synapses. J Neurosci 29:10869–10882.

Amani M, Lauterborn JC, Le AA, Cox BM, Wang W, Quintanilla J, Cox CD, Gall CM, Lynch G (2021) Rapid aging in the perforant path projections to the rodent dentate gyrus. J Neurosci 41:2301–2312.

Andreano JM, Cahill L (2009) Sex influences on the neurobiology of learning and memory. Learn Mem 16:248–266.

Asperholm M, Hogman N, Rafi J, Herlitz A (2019) What did you do yesterday? A meta-analysis of sex differences in episodic memory. Psychol Bull 145:785–821.

Babayan AH, et al. (2012) Integrin dynamics produce a delayed stage of long-term potentiation and memory consolidation. J Neurosci 32:12854–12861.

Baldi P, Vershynin R (2021) A theory of capacity and sparse neural encoding. Neural Netw 143:12–27.

Balthazart J, Baillien M, Ball GF (2006) Rapid control of brain aromatase activity by glutamatergic inputs. Endocrinology 147:359–366.

Barel E, Tzischinsky O (2018) Age and sex differences in verbal and visuospatial abilities. Adv Cogn Psychol 2:51–61.

Bartsch T, Dohring J, Rohr A, Jansen O, Deuschl G (2011) CA1 neurons in the human hippocampus are critical for autobiographical memory, mental time travel, and autonoetic consciousness. Proc Natl Acad Sci U S A 108:17562–17567.

Baudry M, Kramar E, Xu X, Zadran H, Moreno S, Lynch G, Gall C, Bi X (2012) Ampakines promote spine actin polymerization, long-term potentiation, and learning in a mouse model of Angelman syndrome. Neurobiol Dis 47:210–215.

Berlyne DE (1950) Novelty and curiosity as determinants of exploratory behaviour. B J Psychol Gen Sect 41:68–80.

Birnbaum JH, Bali J, Rajendran L, Nitsch RM, Tackenberg C (2015) Calcium flux-independent NMDA receptor activity is required for abeta oligomer-induced synaptic loss. Cell Death Dis 6:e1791.

Blystone SD (2004) Integrating an integrin: a direct route to actin. Biochim Biophys Acta 1692:47–54.

Bosch M, Castro J, Saneyoshi T, Matsuno H, Sur M, Hayashi Y (2014) Structural and molecular remodeling of dendritic spine substructures during long-term potentiation. Neuron 82:444–459.

Bramham CR (2008) Local protein synthesis, actin dynamics, and LTP consolidation. Curr Opin Neurobiol 18:524–531.

Brunetti V, Soda T, Berra-Romani R, De Sarro G, Guerra G, Scarpellino G, Moccia F (2024) Two signaling modes are better than one: flux-independent signaling by ionotropic glutamate receptors is coming of age. Biomedicines 12.

Carlisle HJ, Manzerra P, Marcora E, Kennedy MB (2008) SynGAP regulates steady-state and activity-dependent phosphorylation of cofilin. J Neurosci 28:13673–13683.

Chavez J, Le AA, Quintanilla J, Tagne AM, Piomelli D, Lynch G (2022) Microglia depletion selectively eliminates a singular form of hippocampal long-term potentiation. BioRxiv.

Chen LY, Rex CS, Babayan AH, Kramar EA, Lynch G, Gall CM, Lauterborn JC (2010b) Physiological activation of synaptic Rac> PAK (p-21 activated kinase) signaling is defective in a mouse model of fragile X syndrome. J Neurosci 30:10977–10984.

Chen LY, Rex CS, Casale MS, Gall CM, Lynch G (2007) Changes in synaptic-morphology accompany actin signaling during LTP. J Neurosci 27:5363–5372.

Chen LY, Rex CS, Sanaiha Y, Lynch G, Gall CM (2010a) Learning induces neurotrophin signaling at hippocampal synapses. Proc Natl Acad Sci U S A 107:7030–7035.

Coan EJ, Saywood W, Collingridge GL (1987) MK-801 blocks NMDA receptor-mediated synaptic transmission and long term potentiation in rat hippocampal slices. Neurosci Lett 80:111–114.

Copenhaver AE, LeGates TA (2024) Sex-Specific mechanisms underlie long-term potentiation at hippocampus–>medium spiny neuron synapses in the medial shell of the nucleus accumbens. J Neurosci 44:1–13.

Cox BM, Cox CD, Gunn BG, Le AA, Inshishian VC, Gall CM, Lynch G (2019) Acquisition of temporal order requires an intact CA3 commissural/associational (C/A) feedback system in mice. Commun Biol 2:251.

Cox CD, Rex CS, Palmer LC, Babayan AH, Pham DT, Corwin SD, Trieu BH, Gall CM, Lynch G (2014) A map of LTP-related synaptic changes in dorsal hippocampus following unsupervised learning. J Neurosci 34:3033–3041.

Dede AJ, Frascino JC, Wixted JT, Squire LR (2016) Learning and remembering real-world events after medial temporal lobe damage. Proc Natl Acad Sci U S A 113:13480–13485.

Dere E, Huston JP, De Souza Silva MA (2005a) Episodic-like memory in mice: simultaneous assessment of object, place and temporal order memory. Brain Res Brain Res Protoc 16:10–19.

Dere E, Huston JP, De Souza Silva MA (2005b) Integrated memory for objects, places, and temporal order: evidence for episodic-like memory in mice. Neurobiol Learn Mem 84:214–221.

Dong B, Yue Y, Dong H, Wang Y (2023) N-methyl-D-aspartate receptor hypofunction as a potential contributor to the progression and manifestation of many neurological disorders. Front Mol Neurosci 16:1174738.

Dore K, Aow J, Malinow R (2015) Agonist binding to the NMDA receptor drives movement of its cytoplasmic domain without ion flow. Proc Natl Acad Sci U S A 112:14705–14710.

Dore K, Aow J, Malinow R (2016) The emergence of NMDA receptor metabotropic function: insights from imaging. Front Synaptic Neurosci 8:20.

Dore K, Stein IS, Brock JA, Castillo PE, Zito K, Sjostrom PJ (2017) Unconventional NMDA receptor signaling. J Neurosci 37:10800–10807.

Eacott MJ, Easton A (2010) Episodic memory in animals: remembering which occasion. Neuropsychologia 48:2273–2280.

Ekstrom AD, Ranganath C (2018) Space, time, and episodic memory: the hippocampus is all over the cognitive map. Hippocampus 28:680–687.

El Gaamouch F, Buisson A, Moustie O, Lemieux M, Labrecque S, BontempiB, De Koninck P, Nicole O (2012) Interaction between alphaCaMKII and GluN2B controls ERK-dependent plasticity. J Neurosci 32:10767–10779.

Fischer G, Mutel V, Trube G, Malherbe P, Kew JN, Mohacsi E, Heitz MP, Kemp JA (1997) Ro 25-6981, a highly potent and selective blocker of N-methyl-D-aspartate receptors containing the NR2B subunit. Characterization in vitro. J Pharmacol Exp Ther 283:1285–1292.

Foster KA, McLaughlin N, Edbauer D, Phillips M, Bolton A, Constantine-Paton M, Sheng M (2010) Distinct roles of NR2A and NR2B cytoplasmic tails in long-term potentiation. J Neurosci 30:2676–2685.

Frankiewicz T, Potier B, Bashir ZI, Collingridge GL, Parsons CG (1996) Effects of memantine and MK-801 on NMDA-induced currents in cultured neurones and on synaptic transmission and LTP in area CA1 of rat hippocampal slices. Br J Pharmacol 117:689–697.
Gall CM, Le AA, Lynch G (2021) Sex differences in synaptic plasticity underlying learning. J Neurosci Res 101:764–782.
Gall CM, Le AA, Lynch G (2024) Contributions of site- and sex-specific LTPs to everyday memory. Philos Trans R Soc Lond B Biol Sci 379:20230223.
Gattas S, Elias GA, Janecek J, Yassa MA, Fortin NJ (2022) Proximal CA1 20–40 Hz power dynamics reflect trial-specific information processing supporting nonspatial sequence memory. Elife 11.
Geiger B, Boujemaa-Paterski R, Winograd-Katz SE, Balan Venghateri J, Chung WL, Medalia O (2023) The actin network interfacing diverse integrin-mediated adhesions. Biomolecules 13.
Gogos A, Kwek P, van den Buuse M (2012) The role of estrogen and testosterone in female rats in behavioral models of relevance to schizophrenia. Psychopharmacology 219:213–224.
Granger AJ, Nicoll RA (2014) Expression mechanisms underlying long-term potentiation: a postsynaptic view, 10 years on. Philos Trans R Soc Lond B Biol Sci 369:20130136.
Gray JA, Zito K, Hell JW (2016) Non-ionotropic signaling by the NMDA receptor: controversy and opportunity. F1000Res 5:F1000 Faculty Rev-1010.
Hanson JE, Weber M, Meilandt WJ, Wu T, Luu T, Deng L, Shamloo M, Sheng M, Scearce-Levie K, Zhou Q (2013) Glun2b antagonism affects interneurons and leads to immediate and persistent changes in synaptic plasticity, oscillations, and behavior. Neuropsychopharmacology 38:1221–1233.
Hayashi Y, Shi SH, Esteban JA, Piccini A, Poncer JC, Malinow R (2000) Driving AMPA receptors into synapses by LTP and CaMKII: requirement for GluR1 and PDZ domain interaction. Science 287:2262–2267.
Hebb DO (1949) *The organization of behavior*. New York: Wiley.
Herlitz A, Airaksinen E, Nordstrom E (1999) Sex differences in episodic memory: the impact of verbal and visuospatial ability. Neuropsychology 13:590–597.
Hojo Y, Kawato S (2018) Neurosteroids in adult hippocampus of male and female rodents: biosynthesis and actions of sex steroids. Front Endocrinol 9:183.
Huang CC, Hsu KS (2001) Progress in understanding the factors regulating reversibility of long-term potentiation. Rev Neurosci 12:51–68.
Jain A, Huang GZ, Woolley CS (2019) Latent sex differences in molecular signaling that underlies excitatory synaptic potentiation in the hippocampus. J Neurosci 39:1552–1565.
Jensen A, Theriault K, Yilmaz E, Pon E, Davidson PSR (2023) Mental rotation, episodic memory, and executive control: possible effects of biological sex and oral contraceptive use. Neurobiol Learn Mem 198:107720.
Karakas E, Simorowski N, Furukawa H (2011) Subunit arrangement and phenylethanolamine binding in GluN1/GluN2B NMDA receptors. Nature 475:249–253.
Kelly MT, Yao Y, Sondhi R, Sacktor TC (2007) Actin polymerization regulates the synthesis of PKMzeta in LTP. Neuropharmacology 52:41–45.
Kessels HW, Nabavi S, Malinow R (2013) Metabotropic NMDA receptor function is required for β-amyloid-induced synaptic depression. Proc Natl Acad Sci U S A 110:4033–4038.
Koleske AJ (2013) Molecular mechanisms of dendrite stability. Nat Rev Neurosci 14:536–550.
Kouvaros S, Papatheodoropoulos C (2016) Theta burst stimulation-induced LTP: differences and similarities between the dorsal and ventral CA1 hippocampal synapses. Hippocampus 26:1542–1559.
Kramár EA, Chen LY, Brandon NJ, Rex CS, Liu F, Gall CM, Lynch G (2009) Cytoskeletal changes underlie estrogen's acute effects on synaptic transmission and plasticity. J Neurosci 29:12982–12993.
Kramár EA, Lin B, Rex CS, Gall CM, Lynch G (2006) Integrin-driven actin polymerization consolidates long-term potentiation. Proc Natl Acad Sci U S A 103:5579–5584.
Kramer JH, Delis DC, Kaplan E, O'Donnell L, Prifitera A (1997) Developmental sex differences in verbal learning. Neuropsychology 11:577–584.
Krapivinsky G, Medina I, Krapivinsky L, Gapon S, Clapham DE (2004) SynGAP-MUPP1-CaMKII synaptic complexes regulate p38 MAP kinase activity and NMDA receptor-dependent synaptic AMPA receptor potentiation. Neuron 43:563–574.
Krucker T, Siggins GR, Halpain S (2000) Dynamic actin filaments are required for stable long-term potentiation (LTP) in area CA1 of the hippocampus. Proc Natl Acad Sci USA 97:6856–6861.
Larson J, Lynch G (1988) Role of N-methyl-D-aspartate receptors in the induction of synaptic potentiation by burst stimulation patterned after the hippocampal theta-rhythm. Brain Res 441:111–118.
Larson J, Wong D, Lynch G (1986) Patterned stimulation at the theta frequency is optimal for the induction of hippocampal long-term potentiation. Brain Res 368:347–350.
Larson J, Xiao P, Lynch G (1993) Reversal of LTP by theta frequency stimulation. Brain Res 600:97–102.
Le AA, Lauterborn JC, Jia Y, Wang W, Cox CD, Gall CM, Lynch G (2022b) Prepubescent female rodents have enhanced hippocampal LTP and learning relative to males, reversing in adulthood as inhibition increases. Nat Neurosci 25:180–190.
Le AA, Quintanilla J, Amani M, Piomelli D, Lynch G, Gall CM (2022a) Persistent sexually dimorphic effects of adolescent THC exposure on hippocampal synaptic plasticity and episodic memory in rodents. Neurobiol Dis 162:105565.
Li LJ, et al. (2016) Glycine potentiates AMPA receptor function through metabotropic activation of GluN2A-containing NMDA receptors. Front Mol Neurosci 9:102.
Li Y, et al. (2022) Treatment of cerebral ischemia through NMDA receptors: metabotropic signaling and future directions. Front Pharmacol 13:831181.
Lin B, Kramár EA, Bi X, Brucher FA, Gall CM, Lynch G (2005) Theta stimulation polymerizes actin in dendritic spines of hippocampus. J Neurosci 25:2062–2069.
Lisman J, Grace AA, Duzel E (2011) A neoHebbian framework for episodic memory; role of dopamine-dependent late LTP. Trends Neurosci 34:536–547.
Lisman J, Yasuda R, Raghavachari S (2012) Mechanisms of CaMKII action in long-term potentiation. Nat Rev Neurosci 13:169–182.
Lynch G, Baudry M (1984) The biochemistry of memory: a new and specific hypothesis. Science 224:1057–1063.
Lynch G, Baudry M (2015) Brain and memory: old arguments and new perspectives. Brain Res 1621:1–4.
Lynch G, Kramar EA, Babayan AH, Rumbaugh G, Gall CM (2013) Differences between synaptic plasticity thresholds result in new timing rules for maximizing long-term potentiation. Neuropharmacology 64:27–36.
Lynch G, Kramar EA, Rex CS, Jia Y, Chappas D, Gall CM, Simmons DA (2007) Brain-derived neurotrophic factor restores synaptic plasticity in a knock-in mouse model of Huntington's disease. J Neurosci 27:4424–4434.
Lynch G, Larson J, Kelso S, Barrionuevo G, Schottler F (1983) Intracellular injections of EGTA block induction of hippocampal long-term potentiation. Nature 305:719–721.
Malenka RC, Kauer JA, Zucker RS, Nicoll RA (1988) Postsynaptic calcium is sufficient for potentiation of hippocampal synaptic transmission. Science 242:81–84.
Markram H, Gerstner W, Sjostrom PJ (2011) A history of spike-timing-dependent plasticity. Front Synaptic Neurosci 3:4.
Mielnik CA, et al. (2021) Consequences of NMDA receptor deficiency can be rescued in the adult brain. Mol Psychiatry 26:2929–2942.
Miwa H, Fukaya M, Watabe AM, Watanabe M, Manabe T (2008) Functional contributions of synaptically localized NR2B subunits of the NMDA receptor to synaptic transmission and long-term potentiation in the adult mouse CNS. J Physiol 586:2539–2550.
Nabavi S, Kessels HW, Alfonso S, Aow J, Fox R, Malinow R (2013) Metabotropic NMDA receptor function is required for NMDA receptor-dependent long-term depression. Proc Natl Acad Sci U S A 110:4027–4032.
Naftolin F, Horvath TL, Jakab RL, Leranth C, Harada N, Balthazart J (1996) Aromatase immunoreactivity in axon terminals of the vertebrate brain. an immunocytochemical study on quail, rat, monkey and human tissues. Neuroendocrinology 63:149–155.
Nebieridze N, Zhang XL, Chachua T, Velisek L, Stanton PK, Veliskova J (2012) β-Estradiol unmasks metabotropic receptor-mediated metaplasticity of NMDA receptor transmission in the female rat dentate gyrus. Psychoneuroendocrinology 37:1845–1854.
Noulhiane M, Piolino P, Hasboun D, Clemenceau S, Baulac M, Samson S (2007) Autobiographical memory after temporal lobe resection: neuropsychological and MRI volumetric findings. Brain 130:3184–3199.
Ortega-Carrion A, Feo-Lucas L, Vicente-Manzanares M (2016) Cell migration. In: *Encyclopedia of cell biology* (Bradshaw RA, Stahl PD, eds), Ed 2, pp 247–259. Oxford: Academic Press.

Otto T, Eichenbaum H, Wiener SI, Wible CG (1991) Learning-related patterns of CA1 spike trains parallel stimulation parameters optimal for inducing hippocampal long-term potentiation. Hippocampus 1:181–192.
Paoletti P, Bellone C, Zhou Q (2013) NMDA receptor subunit diversity: impact on receptor properties, synaptic plasticity and disease. Nat Rev Neurosci 14: 383–400.
Papatheodoropoulos C, Kouvaros S (2016) High-frequency stimulation-induced synaptic potentiation in dorsal and ventral CA1 hippocampal synapses: the involvement of NMDA receptors, mGluR5, and (L-type) voltage-gated calcium channels. Learn Mem 23:460–464.
Pospich S, Merino F, Raunser S (2020) Structural effects and functional implications of phalloidin and jasplakinolide binding to actin filaments. Structure 28:437–449.e5.
Rajani V, Sengar AS, Salter MW (2021) Src and Fyn regulation of NMDA receptors in health and disease. Neuropharmacology 193:108615.
Ramachandran B, Frey JU (2009) Interfering with the actin network and its effect on long-term potentiation and synaptic tagging in hippocampal CA1 neurons in slices in vitro. J Neurosci 29:12167–12173.
Rauner C, Köhr G (2011) Triheteromeric NR1/NR2A/NR2B receptors constitute the major N-methyl-D-aspartate receptor population in adult hippocampal synapses. J Biol Chem 286:7558–7566.
Raymond CR (2007) LTP forms 1, 2 and 3: different mechanisms for the "long" in long-term potentiation. Trends Neurosci 30:167–175.
Rehnman J, Herlitz A (2007) Women remember more faces than men do. Acta Psychol 124:344–355.
Rex CS, et al. (2010) Myosin IIb regulates actin dynamics during synaptic plasticity and memory formation. Neuron 67:603–617.
Rex CS, Chen LY, Sharma A, Liu J, Babayan AH, Gall CM, Lynch G (2009) Different Rho GTPase-dependent signaling pathways initiate sequential steps in the consolidation of long-term potentiation. J Cell Biol 186:85–97.
Rex CS, Lin CY, Kramár EA, Chen LY, Gall CM, Lynch G (2007) Brain-derived neurotrophic factor promotes long-term potentiation-related cytoskeletal changes in adult hippocampus. J Neurosci 27:3017–3029.
Ryan TJ, et al. (2013) Evolution of GluN2A/B cytoplasmic domains diversified vertebrate synaptic plasticity and behavior. Nat Neurosci 16:25–32.
Scanlon DP, Bah A, Krzeminski M, Zhang W, Leduc-Pessah HL, Dong YN, Forman-Kay JD, Salter MW (2017) An evolutionary switch in ND2 enables Src kinase regulation of NMDA receptors. Nat Commun 8:15220.
Scharfman HE, MacLusky NJ (2006) Estrogen and brain-derived neurotrophic factor (BDNF) in hippocampus: complexity of steroid hormone-growth factor interactions in the adult CNS. Front Neuroendocrinol 27:415–435.
Seeburg PH, Burnashev N, Kohr G, Kuner T, Sprengel R, Monyer H (1995) The NMDA receptor channel: molecular design of a coincidence detector. Recent Prog Horm Res 50:19–34.
Seese RR, Babayan AH, Katz AM, Cox CD, Lauterborn JC, Lynch G, Gall CM (2012) LTP induction translocates cortactin at distant synapses in wild-type but not Fmr1 knock-out mice. J Neurosci 32:7403–7413.
Seese RR, Chen LY, Cox CD, Schulz D, Babayan AH, Bunney WE, Henn FA, Gall CM, Lynch G (2013) Synaptic abnormalities in the infralimbic cortex of a model of congenital depression. J Neurosci 33:13441–13448.
Seese RR, Wang K, Yao YQ, Lynch G, Gall CM (2014) Spaced training rescues memory and ERK1/2 signaling in fragile X syndrome model mice. Proc Natl Acad Sci U S A 111:16907–16912.
Shipton OA, Paulsen O (2014) Glun2a and GluN2B subunit-containing NMDA receptors in hippocampal plasticity. Philos Trans R Soc Lond B Biol Sci 369:20130163.
Smith CC, Smith LA, Bredemann TM, McMahon LL (2016) 17beta estradiol recruits GluN2B-containing NMDARs and ERK during induction of long-term potentiation at temporoammonic-CA1 synapses. Hippocampus 26:110–117.
Smith CC, Vedder LC, McMahon LL (2009) Estradiol and the relationship between dendritic spines, NR2B containing NMDA receptors, and the magnitude of long-term potentiation at hippocampal CA3-CA1 synapses. Psychoneuroendocrinology 34:S130–142.
Song X, Jensen MO, Jogini V, Stein RA, Lee CH, McHaourab HS, Shaw DE, Gouaux E (2018) Mechanism of NMDA receptor channel block by MK-801 and memantine. Nature 556:515–519.
Staubli U, Lynch G (1987) Stable hippocampal long-term potentiation elicited by 'theta' pattern stimulation. Brain Res 435:227–234.
Stein IS, Gray JA, Zito K (2015) Non-Ionotropic NMDA receptor signaling drives activity-induced dendritic spine shrinkage. J Neurosci 35:12303–12308.
Stein IS, Park DK, Claiborne N, Zito K (2021) Non-ionotropic NMDA receptor signaling gates bidirectional structural plasticity of dendritic spines. Cell Rep 34:108664.
Sun Y, Xu Y, Cheng X, Chen X, Xie Y, Zhang L, Wang L, Hu J, Gao Z (2018) The differences between GluN2A and GluN2B signaling in the brain. J Neurosci Res 96:1430–1443.
Tang DD, Anfinogenova Y (2008) Physiologic properties and regulation of the actin cytoskeleton in vascular smooth muscle. J Cardiovasc Pharmacol Ther 13:130–140.
Tang B, Ji Y, Traub RJ (2008) Estrogen alters spinal NMDA receptor activity via a PKA signaling pathway in a visceral pain model in the rat. Pain 137: 540–549.
Tullis JE, Bayer KU (2023) Distinct synaptic pools of DAPK1 differentially regulate activity-dependent synaptic CaMKII accumulation. iScience 26: 106723.
Tulving E (1984) *Elements of episodic memory*. Oxford: Oxford University Press.
Tuscher JJ, Fortress AM, Kim J, Frick KM (2015) Regulation of object recognition and object placement by ovarian sex steroid hormones. Behav Brain Res 285:140–157.
Ueda HH, Nagasawa Y, Sato A, Onda M, Murakoshi H (2022) Chronic neuronal excitation leads to dual metaplasticity in the signaling for structural long-term potentiation. Cell Rep 38:110153.
Umbach G, Kantak P, Jacobs J, Kahana M, Pfeiffer BE, Sperling M, Lega B (2020) Time cells in the human hippocampus and entorhinal cortex support episodic memory. Proc Natl Acad Sci U S A 117:28463–28474.
Vanderklish P, Bednarski E, Lynch G (1996) Translational suppression of calpain blocks long-term potentiation. Learn Mem 3:209–217.
Vierk R, et al. (2012) Aromatase inhibition abolishes LTP generation in female but not in male mice. J Neurosci 32:8116–8126.
Volianskis A, Bannister N, Collett VJ, Irvine MW, Monaghan DT, Fitzjohn SM, Jensen MS, Jane DE, Collingridge GL (2013) Different NMDA receptor subtypes mediate induction of long-term potentiation and two forms of short-term potentiation at CA1 synapses in rat hippocampus in vitro. J Physiol 591:955–972.
Voyer D, Saint Aubin J, Altman K, Gallant G (2021) Sex differences in verbal working memory: a systematic review and meta-analysis. Psychol Bull 147:352–398.
Wang W, Cox BM, Jia Y, Le AA, Cox CD, Jung KM, Hou B, Piomelli D, Gall CM, Lynch G (2018b) Treating a novel plasticity defect rescues episodic memory in Fragile X model mice. Mol Psychiatry 23:1798–1806.
Wang W, Le AA, Hou B, Lauterborn JC, Cox CD, Levin ER, Lynch G, Gall CM (2018a) Memory-related synaptic plasticity is sexually dimorphic in rodent hippocampus. J Neurosci 38:7935–7951.
Wang H, Peng RY (2016) Basic roles of key molecules connected with NMDAR signaling pathway on regulating learning and memory and synaptic plasticity. Mil Med Res 3:26.
Waters EM, Mazid S, Dodos M, Puri R, Janssen WG, Morrison JH, McEwen BS, Milner TA (2019) Effects of estrogen and aging on synaptic morphology and distribution of phosphorylated Tyr1472 NR2B in the female rat hippocampus. Neurobiol Aging 73:200–210.
Weilinger NL, et al. (2016) Metabotropic NMDA receptor signaling couples Src family kinases to pannexin-1 during excitotoxicity. Nat Neurosci 19: 432–442.
Wickens MM, Bangasser DA, Briand LA (2018) Sex differences in psychiatric disease: a focus on the glutamate system. Front Mol Neurosci 11:197.
Wong JM, Gray JA (2018) Long-term depression is independent of GluN2 subunit composition. J Neurosci 38:4462–4470.
Youngjohn JR, Larrabee GJ, Crook TH (1991) First-last names and the grocery list selective reminding test: two computerized measures of everyday verbal learning. Arch Clin Neuropsychol 6:287–300.
Zhou Q, Sheng M (2013) NMDA receptors in nervous system diseases. Neuropharmacology 74:69–75.
Zhu G, Liu Y, Wang Y, Bi X, Baudry M (2015) Different patterns of electrical activity lead to long-term potentiation by activating different intracellular pathways. J Neurosci 35:621–633.